

การพัฒนาวิธีการตรวจวัดไอโอไดด์ไอออนในไข่ด้วยเทคนิคทางเคมีไฟฟ้า

นางสาวปิยะดา สุวรรณดิษฐากุล

สถาบันวิทยบริการ

จุฬาลงกรณ์มหาวิทยาลัย

วิทยานิพนธ์นี้เป็นส่วนหนึ่งของการศึกษาตามหลักสูตรปริญญาวิทยาศาสตรมหาบัณฑิต

สาขาวิชาเคมี ภาควิชาเคมี

คณะวิทยาศาสตร์ จุฬาลงกรณ์มหาวิทยาลัย

ปีการศึกษา 2549

ลิขสิทธิ์ของจุฬาลงกรณ์มหาวิทยาลัย

METHOD DEVELOPMENT FOR DETERMINATION OF IODIDE ION IN EGG USING
ELECTROCHEMICAL TECHNIQUES



MISS PIYADA SUWANDITTAKUL

สถาบันวิทยบริการ
จุฬาลงกรณ์มหาวิทยาลัย

A Thesis Submitted in Partial Fulfillment of the Requirements
for the Degree of Master of Science Program in Chemistry

Department of Chemistry

Faculty of Science

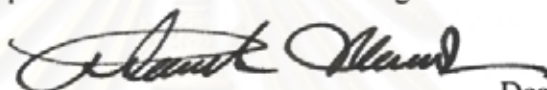
Chulalongkorn University

Academic Year 2006

Copyright of Chulalongkorn University


Thesis Title	Method development for determination of iodide ion in egg using electrochemical techniques
By	Miss Piyada Suwandittakul
Field of Study	Chemistry
Thesis Advisor	Pakorn Varanusupakul, Ph.D.
Thesis Co-advisor	Associate Professor Orawon Chailapakul, Ph.D.

Accepted by the Faculty of Science, Chulalongkorn University in Partial Fulfillment of the Requirements for the Master's Degree



..... Dean of the the Faculty of Science
(Professor Piamsak Menasveta, Ph.D.)

THESIS COMMITTEE



..... Chairman
(Associate Professor Sirirat Kokpol, Ph.D.)



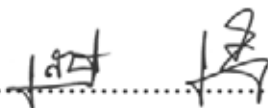
..... Thesis Advisor
(Pakorn Varanusupakul, Ph.D.)



..... Thesis Co-advisor
(Associate Professor Orawon Chailapakul, Ph.D.)



..... Member
(Assistant Professor Wanlapa Acungmaitepirom, Ph.D.)



..... Member
(Assistant Professor Saowarux Fuangswasdi, Ph.D.)

ปิยะดา สุวรรณดิษฐากุล: การพัฒนาวิธีตรวจวัดไอโอดีนไอออนในไข่ด้วยเทคนิคทางเคมีไฟฟ้า (METHOD DEVELOPMENT FOR DETERMINATION OF IODIDE ION IN EGG USING ELECTROCHEMICAL TECHNIQUES)

อ.ที่ปรึกษา: ดร.ปกรณ วรานุศูภากุล, อ.ที่ปรึกษาร่วม: รศ.ดร.อรรพรรณ ชัยลภากุล 78 หน้า.

งานวิจัยนี้ได้พัฒนาเทคนิคการตรวจวัดทางเคมีไฟฟ้าร่วมกับระบบโพลีวินเจคชัน เพื่อวิเคราะห์หาปริมาณไอโอดีนไอออนในไข่ ทำการศึกษาปฏิกิริยาออกซิเดชันของไอโอดีนไอออน โดยใช้เทคนิคไซคลิกโวลแทมเมตรีเปรียบเทียบระหว่างขั้วไฟฟ้าเพชรที่โคปด้วยโบรอนและขั้วไฟฟ้ากลาสสิคาร์บอนในสารละลายฟอสเฟตบัฟเฟอร์ ค่าพีเอช 5 เข้มข้น 60 มิลลิโมลาร์ พบว่าขั้วไฟฟ้าทั้งสองชนิดให้ผลของไซคลิกโวลแทมเมแกรมของไอโอดีนไอออนที่ชัดเจน แต่ที่ขั้วไฟฟ้าเพชรที่โคปด้วยโบรอนให้สัญญาณพื้นหลังต่ำกว่าขั้วไฟฟ้ากลาสสิคาร์บอน งานวิจัยนี้เลือกขั้วไฟฟ้าเพชรที่โคปด้วยโบรอนเป็นขั้วไฟฟ้าใช้งาน นอกจากนี้ยังได้ศึกษาการนำวิธีการให้สัญญาณกระตุ้นแบบพัลส์มาใช้ในการตรวจวัดแบบแอมเพอโรเมตรี เพื่อเป็นการปรับปรุงความคงทนของสัญญาณซึ่งอาจมีผลจากการดูดซับของสปีชีส์ที่เกิดจากปฏิกิริยาเคมีไฟฟ้าที่ผิวหน้าขั้วไฟฟ้า ตัวแปรที่เหมาะสมของการให้สัญญาณกระตุ้นแบบพัลส์ได้แก่ ศักย์ไฟฟ้าตรวจวัดที่ 0.8 โวลต์เป็นเวลา 60 มิลลิวินาที ศักย์ไฟฟ้าออกซิเดชันที่ 1.2 โวลต์เป็นเวลา 700 มิลลิวินาที และศักย์ไฟฟารีดักชันที่ 1.1 โวลต์เป็นเวลา 30 มิลลิวินาที วิธีการตรวจวัดด้วยระบบโพลีวินเจคชัน-พัลส์แอมเพอโรเมทรินั้นใช้สารละลายฟอสเฟตบัฟเฟอร์ความเข้มข้น 60 มิลลิโมลาร์ ค่าพีเอช 5 อัตราการไหล 1 มิลลิลิตรต่อนาที ณ อุณหภูมิห้อง การประเมินวิธีการตรวจวัดในช่วงความเข้มข้นในการตรวจวัดที่เป็นเส้นตรงระหว่าง 50 ถึง 2000 ไมโครกรัมต่อลิตร ซีดจำกัดต่ำสุดในการตรวจวัดที่ 5.4 ไมโครกรัมต่อลิตร ซีดจำกัดต่ำสุดในการวิเคราะห์ปริมาณที่ 16.5 ไมโครกรัมต่อลิตร และค่าการคืนกลับ 114 เปอร์เซ็นต์ที่ค่าเบี่ยงเบนมาตรฐานสัมพัทธ์ 6 เปอร์เซ็นต์ ได้พยายามนำวิธีการนี้ไปใช้วิเคราะห์ไอโอดีนในไข่ตัวอย่าง หลังจากการทำอัลคาไลน์ดรายแอสซิง พบว่ามีปัญหากับเมทริกซ์ที่ไม่เหมาะสมกับระบบทางเคมีไฟฟ้า จึงได้นำเทคนิคการดึงตัวอย่างไมโครไดอะไลซิสมาใช้ดึงไอโอดีนไอออนจากตัวอย่างไข่ จากผลการวิเคราะห์ปริมาณไอโอดีนในไข่เบื้องต้นระหว่างวิธีการดึงตัวอย่างไมโครไดอะไลซิสร่วมกับการตรวจวัดด้วยระบบโพลีวินเจคชัน-พัลส์แอมเพอโรเมตรี (1.06 ไมโครกรัมต่อกรัมไข่ ที่ค่าเบี่ยงเบนมาตรฐานสัมพัทธ์ 6 เปอร์เซ็นต์) และวิธีการเตรียมตัวอย่างอัลคาไลน์ดรายแอสซิงร่วมกับวิธีแคตตะไลติกคัลเลอรีเมตรี (1.11 ไมโครกรัมต่อกรัมไข่ ที่ค่าเบี่ยงเบนมาตรฐาน 0.1 เปอร์เซ็นต์) ให้ผลที่ใกล้เคียงกัน

ภาควิชา.....เคมี..... ลายมือชื่อนิสิต..... ปิยะดา สุวรรณดิษฐากุล
สาขาวิชา.....เคมี..... ลายมือชื่ออาจารย์ที่ปรึกษา.....
ปีการศึกษา...2549..... ลายมือชื่ออาจารย์ที่ปรึกษาร่วม.....

4772379523 : MAJOR CHEMISTRY

KEY WORD: IODIDE ION / PULSED AMPEROMETRIC DETECTION / BORON-DOPED DIAMOND

PIYADA SUWANDITTAKUL : METHOD DEVELOPMENT FOR DETERMINATION OF IODIDE ION IN EGG USING ELECTROCHEMICAL TECHNIQUES. THESIS ADVISOR: PAKORN VARANUSUPAKUL, Ph.D., THESIS COADVISOR: ASSOC.PROF.ORAWAN CHAILAPAKUL, Ph.D., 78 pp.

The electrochemical detection with flow injection (FI) system was developed for the determination of iodide ion in egg samples. The oxidation potential of iodide was investigated using cyclic voltammetry (CV) in 60 mM phosphate buffer (pH 5). The experiments were compared between using boron-doped diamond (BDD) and using glassy carbon electrodes (GC). It was found that both electrodes provided well-defined cyclic voltammograms. However, the background current of BDD electrode was much lower than the background current of GC electrode. The BDD electrode was selected as working electrode for this work. The pulsed potential waveform was also studied and applied with flow injection amperometric detection in order to improve the stability of the signal that might be affected by the adsorption of electrochemical species at the electrode surface. The optimized pulsed potential waveform parameters were 0.8 V detection potential; 30 msec delay time; 30 msec integration time; 1.2 V oxidation potential; 700 msec oxidation time; 1.1 V reduction potential; and 30 msec reduction time. The FI-PAD-BDD was carried out in 60 mM phosphate buffer pH 5 at flow rate of 1 ml/min. The method was evaluated with standard iodide. The linear dynamic range was 50 to 2000 $\mu\text{g/L}$. The limit of detection and the limit of quantitation were 5.4 $\mu\text{g/L}$ and 16.5 $\mu\text{g/L}$, respectively. The recovery was 114% with 6% RSD. The method was intended to apply for determination of iodide in egg sample after alkali dry ashing; however, there was a problem with the incompatibility of the matrix to the electrochemical system. Alternatively, microdialysis sampling was attempted in order to retrieve iodide ion from egg samples. The preliminary results of iodide in egg samples obtained from both microdialysis with FI-PAD-BDD method (1.06 $\mu\text{g/g}$ of egg with 6%RSD) and alkali dry ashing with catalytic colorimetric method (1.11 $\mu\text{g/g}$ of egg with 0.1%RSD) were comparable.

Department.....CHEMISTRY.....Student's signature.....*Piyada Suwandittakul*
 Field of study.....CHEMISTRY..... Advisor's signature.....*Pakorn Varanusupakul*
 Academic year....2006..... Co-advisor's signature.....*Orawan Chailapakul*

ACKNOWLEDGEMENTS

The success of this research can be attributed to the extensive support and assistance from my advisor, Dr. Pakorn Varanusupakul and my co-advisor, Associate Dr. Professor Orawon Chailapakul, for suggestions, assistance and encouragement. In addition, I would like to extend my appreciation to Associate Professor Dr. Sirirat Kokpol, Assistant Professor Dr. Wanlapa Aeungmaitrepirom, and Assistant Professor Dr. Saowarux Fuangswasdi for their valuable suggestions as my thesis committees.

This work cannot be completed without kindness and helps of many people. I would like to thank Lecturer. Ponwason Eamchan, Dr. Passapol Ngamokot and Miss Anchana Preechaworapun for their suggestions and helps. Next, I would like to thank all of many people in Environmental analysis research unit and Electrochemical research group for their friendship and the good supports. My thank is also extended to Thesis Support Fund, Graduate School Chulalongkorn University.

Finally, I am grateful to my family for their support, care, encourage and love.

สถาบันวิทยบริการ
จุฬาลงกรณ์มหาวิทยาลัย

CONTENTS

	PAGE
ABSTRACT (IN THAI)	iv
ABSTRACT (IN ENGLISH).....	v
ACKNOWLEDGEMEN.....	vi
CONTENTS.....	vii
LIST OF TABLES	xi
LIST OF FIGURES.....	xii
LIST OF SYMBOLS AND ABBREVIATION	xv
CHAPTER I INTRODUCTION	1
CHAPTER II THEORY.....	4
2.1 Electrochemical techniques	4
2.1.1Cyclic voltammetry.....	4
2.1.1.1 Data interpretation	7
2.1.1.1.1 Reversible system	7
2.1.1.1.2 Irreversible and Quasi-Reversible system	9
2.1.1.2 Study of reaction mechanism.....	10
2.1.2 Amperometry	13
2.1.3 Pulsed amperometric detection.....	14
2.2 Flow injection analysis	15
2.3 Determination of iodide in egg	17
CHAPTER III EXPERIMENTAL.....	18
3.1 Instruments and equipments	18
3.1.1 Electrochemical method.....	18
3.1.2 Microdialysis sampling.....	19
3.1.3 Catalytic colorimetric method.....	19
3.2 Chemicals and reagents.....	20
3.3 Electrochemical method.....	20
3.3.1 Preparation of chemical solution	20
3.3.1.1 Phosphate buffer as supporting electrolyte	20
3.3.1.2 Stock standard iodide solution	20

	PAGE
3.3.1.3 Working standard iodide solution.....	21
3.3.2 Cyclic voltammetric study	21
3.3.2.1 Background current	22
3.3.2.2 pH optimization	22
3.3.2.3 Effect of scan rate	22
3.3.3 The flow injection analysis with amperometric detection using boron-doped diamond electrode.....	22
3.3.3.1 Hydrodynamic Voltammetry	22
3.3.3.2 Amperometric detection	23
3.3.3.3 Calibration and linearity for flow injection analysis with amperometric detection using boron-doped diamond electrode.....	25
3.3.3.4 Limit of Detection (LOD) and Limit of Quantitation (LOQ) for flow injection analysis with amperometric detection using boron-doped diamond electrode	25
3.3.3.5 Precision and accuracy for flow injection analysis with amperometric detection using boron-doped diamond electrode.....	25
3.3.4 The flow injection analysis with pulsed amperometric detection using boron-doped diamond electrode (FI-PAD-BDD)	26
3.3.4.1 Pulsed amperometric detection.....	26
3.3.4.2 PAD waveform optimization	26
3.3.4.3 Calibration and linearity for flow injection analysis with pulsed amperometric detection (PAD) using boron-doped diamond electrode (FI-PAD-BDD)	27
3.3.4.4 Limit of Detection (LOD) and Limit of Quantitation (LOQ) for flow injection analysis with pulsed amperometric detection using boron-doped diamond electrode (FI-PAD-BDD).....	27

	PAGE
3.3.4.5 Precision and accuracy for flow injection analysis with pulsed amperometric detection using boron-doped diamond electrode (FI-PAD-BDD)	27
3.4 Catalytic colorimetric method.....	28
3.4.1 Preparation of chemical solutions	28
3.4.1.1 Stock standard iodide solution.....	28
3.4.1.2 Working standard iodide solution.....	28
3.4.1.3 Potassium carbonate solution 30% (m/V)	28
3.4.1.4 Potassium thiocyanate solution 0.0023% (m/V)	28
3.4.1.5 Sodium nitrite solution 2.07% (m/V)	28
3.4.1.6 Ammonium iron(III) sulfate reagent	29
3.4.1.7 Zinc sulfate solution 10% (m/V)	29
3.4.2 Alkali dry ashing.....	29
3.4.3 Catalytic colorimetric method.....	30
3.4.4 Calibration and linearity for catalytic colorimetric method.....	30
3.4.5 Limit of Detection (LOD) and Limit of Quantitation (LOQ) for catalytic colorimetric method.....	30
3.4.6 Precision and accuracy for catalytic colorimetric method	31
3.5 Application of the methods for determination of iodide in egg samples.....	31
CHATER IV RESULTS AND DISCUSSION.....	32
4.1 Electrochemical method.....	32
4.1.1 Cyclic voltammetry study	32
4.1.1.1 Background current	32
4.1.1.2 Optimal pH	34
4.1.1.3 Effect of scan rate	37
4.1.1.4 Flow injection analysis with amperometric detection using boron-doped diamond electrode	39
4.1.1.4.1 Hydrodynamic voltammetry	39

	PAGE
4.1.1.4.2 Method evaluation for flow injection analysis with amperometric detection using boron-doped diamond electrode.....	42
4.1.1.5 Flow injection analysis with pulsed amperometric detection with using boron-doped diamond electrode (FI-PAD-BDD)	43
4.1.1.5.1 Optimal PAD	43
4.1.1.5.2 Method evaluation for flow injection analysis with pulsed amperometric detection with using boron-doped diamond electrode (FI-PAD-BDD)	49
4.2 Catalytic colorimetric method.....	50
4.2.1 Method evaluation for catalytic colorimetric method.....	50
4.3 Application of electrochemical techniques for determination of iodide in egg sample	51
4.3.1 Microdialysis sampling	52
CHAPTER V CONCLUSION AND SUGGESTION FOR FUTURE WORK	55
5.1 Conclusion	55
5.2 Suggestion for future work	56
REFERENCES	57
APPENDICES	61
VITA	78

LIST OF TABLES

TABLE	PAGE
3-1 Optimal PAD waveform parameters for the developed method at the Au electrode and the anodized BDD electrode.....	26
4-1 Optimal PAD waveform parameters for the developed method at the BDD electrode.....	48
4-2 Comparative results of flow injection-electrochemical methods and catalytic colorimetric method for determination of iodide in egg samples.....	53
A-1 The current responds of optimization pH by cyclic voltammetry using BDD Electrode.....	62
A-2 The current responds of optimization pH by cyclic voltammetry using GC Electrode.....	63
A-3 The current responds of varies scan rate at BDD electrode.....	64
A-4 The current responds of varies scan rate at GC electrode.....	65
A-5 The current responds of hydrodynamic voltammetry for FI-amperometry with BDD electrode of 100 mg/L iodide in 60 mM phosphate buffer (pH 5) at various potentials.....	66
A-6 FI-PAD-BDD response as a function of t_{del} for 100 mg/L of iodide at the boron-doped diamond electrode.....	68
A-7 FI-PAD-BDD response as a function of t_{int} for 100 mg/L of iodide at the boron-doped diamond electrode.....	70
A-8 FI-PAD-BDD response as a function of E_{oxd} for 100 mg/L of iodide at the boron-doped diamond electrode.....	71
A-9 FI-PAD-BDD response as a function of t_{oxd} for 100 mg/L of iodide at the boron-doped diamond electrode.....	72
A-10 FI-PAD-BDD response as a function of E_{red} for 100 mg/L of iodide at the boron-doped diamond electrode.....	74
A-11 FI-PAD-BDD response as a function of t_{red} for 100 mg/L of iodide at the boron-doped diamond electrode.....	76

LIST OF FIGURES

FIGURE	PAGE
2-1 Triangular potential waveform in cyclic voltammetry experiment.....	5
2-2 Typical cyclic voltammogram for a reversible $O + ne^- \leftrightarrow R$ redox process	6
2-3 Concentration distribution of the oxidized and reduced forms of the redox couple at different times during a cyclic voltammetric experiment corresponding to the initial potential (a), to the formal potential of the couple during the forward and reverse scans (b,d), and to the achievement of a zero reactant surface concentration (c)	7
2-4 Cyclic voltammograms for irreversible (curve A) and quasi-reversible (curve B) redox processes	9
2-5 Cyclic voltammograms for a reversible electron transfer followed by an irreversible step for various ratios of chemical rate constant to scan rate, k/a , where $a = nFv/RT$	12
2-6 Amperometry (E-t) waveform.....	13
2-7 The three-step PAD waveform	14
2-8 Schematic diagram of the basic FIA where C is carrier, P is pump, S is point of sample injection, RC is reaction coil, D is detector and W is waste	15
2-9 The typical output form of a peak, the recording starting at S (time of injection t_0). H is the peak height, W is the peak width at a selected level, and A is a peak area, T is the residence time corresponding to the peak height measurement, and t_b is the peak width at the baseline	16
3-1 The electrochemical cell for cyclic voltammetry study.....	21
3-2 The FI manifold1 with pulsed amperometric detection (PAD) using BDD as working electrode and 60 mM phosphate buffer at pH 5 as carrier.....	24
3-3 The thin layer Flow cell.....	24
4-1 The overlaid background voltammograms of 60 mM phosphate buffer (pH 5) at BDD electrode (dotted line) and at GC electrode (solid line). The scan rate was 50 mV/s	33
4-2 The cyclic voltammogram of 63.5 mg/L iodide in 60 mM phosphate buffer (pH 5) at BDD electrode. The scan rate was fixed at 50 mV/s.....	35

FIGURE	PAGE
4-3 The cyclic voltammogram of 63.5 mg/L iodide in 60 mM phosphate buffer (pH 5) at GC electrode. The scan rate was 50 mV/s.....	35
4-4 Overlaid cyclic voltammograms of 63.5 mg/L iodide in 60 mM phosphate buffer at BDD electrode were overlaid from pH 3 to pH 8	36
4-5 Overlaid cyclic voltammograms of 63.5 mg/L iodide in 60 mM phosphate buffer at GC electrode were overlaid from pH 3 to pH 8	36
4-6 Cyclic voltammogram for 63.5 mg/L iodide in phosphate buffer (pH 5) at boron-doped diamond electrode for different scan rates of 10, 25, 50, 75, 100, 200, 300, 400 and 500 mV/s	37
4-7 The relationship between the oxidation current and the square root of the scan rates at boron-doped diamond electrode	38
4-8 Cyclic voltammogram for 63.5 mg/L iodide in phosphate buffer (pH 5) at glassy carbon electrode for different scan rates of 10, 25, 50, 75, 100, 200, 300, 400 and 500 mV/s	38
4-9 The relationship between the oxidation current and the square root of the scan rates at glassy carbon electrode	39
4-10 Hydrodynamic voltammograms for 100 mg/L of iodide in 60 mM phosphate buffer (pH 5) at each potential such as 0.3, 0.4, 0.5, 0.6, 0.7, 0.8, 0.9, 1.0, 1.1 and 1.2 V	40
4-11 Hydrodynamic signal of carrier, 60 mM phosphate buffer (pH 5) or the background current and peak current from injection (n=4) of 100 mg/L of iodide into the carrier stream	41
4-12 Plot of the signal-to-background ratio (S/B) and the applied potentials for flow injection with amperometric detection	41
4-13 Linear dynamic range of iodide determined by flow injection analysis with amperometric detection using boron-doped diamond electrode	42
4-14 FI-PAD-BDD response as a function of t_{del} for 100 mg/L of iodide at the boron-doped diamond electrode	44

FIGURE**PAGE**

4-15 FI-PAD-BDD response as a function of t_{int} for 100 mg/L of iodide at the boron-doped diamond electrode	44
4-16 FI-PAD-BDD response as a function of E_{oxd} for 100 mg/L of iodide at the boron-doped diamond electrode	45
4-17 FI-PAD-BDD response as a function of t_{oxd} for 100 mg/L of iodide at the boron-doped diamond electrode	46
4-18 FI-PAD-BDD response as a function of E_{red} for 100 mg/L of iodide at the boron-doped diamond electrode	47
4-19 FI-PAD-BDD response as a function of t_{red} for 100 mg/L of iodide at the boron-doped diamond electrode	47
4-20 The three-step PAD waveform for the determination of iodide ion.....	49
4-21 Linear dynamic range of iodide determined by FI-PAD-BDD	50
4-22 Working range of iodide determined by catalytic colorimetric method.....	51
4-23 Technical setup of hollow fiber membrane microdialysis.....	52

LIST OF SYMBOLS AND ABBREVIATIONS

A	Activity
Abs.	Absorbance
BDD	Boron-doped diamond
C	Chemical reaction
CE	Electrode process involving an chemical reaction followed by electrochemical reaction
E	Electron transfer/ electrochemical Reaction
EC	Electrode process involving an electrochemical reaction followed by chemical reaction
E°	Standard electrode potential
$E_{1/2}$	Half wave potential
E_p	Peak potential
FI	Flow injection
G	Gram
GC	Glassy carbon
hr.	Hour
i_p	Peak current
$i_{p,r}$	Reverse peak current
$i_{p,f}$	Forward peak current
k°	Standard rate constant
L	Liter
LOD	Limit of Detection
LOQ	Limit of Quantitation
O	The oxidized species
PAD	Pulsed amperometric detection

min	Minute
mL	Milliter
mM	Millimole
msec	Millisecond
n, n_a	Number of electrons
rpm	Round per minute
RSD	Relative Standard Deviation
sec	Second
SD	Standard Deviation
UV-Vis	Ultraviolet-visible
V	Volte
μL	Microliter
μg	Microgram
μA	Microampare
α	Transfer coefficient



สถาบันวิทยบริการ
จุฬาลงกรณ์มหาวิทยาลัย

CHAPTER I

INTRODUCTION

Iodine is an essential micronutrient. In food, iodine is present in the forms of iodide salts or iodate salts. Iodine is one of key components of thyroid hormones that play an important role in the development of brain function, cell growth and control the energy metabolism of the body. Deficiency of iodine leads to goiter, irreversible mental retardation and decrease of survival rates among children. Generally, the amount of iodine daily intake of 150 μg of iodide is required for adult but it should not exceed 1 mg of iodide/day (WHO). To prevent iodine deficiency disorder (IDD), many iodine supplement dietaries are available, such as drinking water, tablets, salt, as well as egg. The concentration of iodine in most foods is low therefore accurate determination requires a sensitive analytical method and freedom from contamination.

There are several reports for determination of iodide. The main methods for analysis are chromatography, spectrophotometry, catalytic spectrophotometry and electrochemistry [1-10]. For gas chromatographic method, iodide was oxidized and iodinated using 2-iodosobenzoate and *N,N*-dimethylaniline, respectively, to form 4-iodo-*N,N*-dimethylaniline which would be extracted by solid phase microextraction (SPME) or single drop microextraction (SDME) prior to analysis by gas chromatography-mass spectrometry (GC-MS) [11]. For high-performance liquid chromatography (HPLC), the iodine speciation could be determined directly by combining anion exchange chromatography and spectrophotometry. The method was applied to quantitative determination of iodide and iodate, as the difference of total inorganic iodide and iodide after reduction of the sample by NaHSO_3 , and determination of organic iodine as the difference of total iodide (after organic decomposition by dehydrohalogenation and reduction by NaHSO_3) and total inorganic iodide [12]. GC-MS and HPLC needed some derivatization step that was quite complicated and prone to iodine losses and contamination.

Atomic absorption spectrometry (AAS) has also been applied to the determination of iodide [13]. Iodide was first precipitated as AgI and excess Ag^+ would be determined by flame AAS. Alternatively, iodide was formed complex with

Hg^+ in acid medium and was passed through a cation-exchange resin, where the excess Hg^+ was adsorbed. The Hg^+ bound to I^- was determined by cold vapor AAS. The determination of non-metals, such as halogens, sulfur, oxygen, nitrogen, phosphorous and carbon by AAS involved certain difficulties. Firstly, due to the high energy difference between the lowest excited state and the ground state for non-metals, the short wavelength radiation was needed for the electronic transitions to occur. Thus, the analytical resonance lines of non-metals lay in the shorter wavelength region of the electromagnetic spectrum, so-called vacuum-UV spectral region ranging from 10 to about 180-190 nm. Unfortunately, there was a lack of commercial radiation source that provided these lines, especially for elements of high volatility such as iodine, because it was difficult to ensure the manufacture of reproducible and stable lamps. Moreover, the selection of the analytical line in the spectrophotometer represented another problem because commercial atomic absorption spectrometers were usually equipped with monochromators that covered from near-UV to near-IR region, which was from about 190 to 850 nm. Therefore, the vacuum-UV region lay outside the commercially attainable range of wavelength. Finally, the absorption of analytical radiation by the atmospheric oxygen produced a high absorption background that could make it difficult to attain useful results.

There was a report for determination of iodine using the chemiluminescence (CL) reaction between iodide and luminol, which was carried out in the flow injection system equipped with gas-diffusion membrane (GD) for selective detection at 425 nm [14].

The most commonly used chemical assays have been colorimetric methods that measured the catalytic effect of iodine on the reduction of Ce^{+4} by As^{+3} (Ce-As) [15] or the destruction of iron(III)-thiocyanate by nitrite (Thio-Nit or Sveikina method) [16-17]. Comparisons were made on two manual colorimetric iodine assays [18]. The Thio-Nit assay was more sensitive. The correlation, r , for the Thio-Nit assay was also greater, (0.990 for 0-6 ng/mL), when compared with the Ce-As assay (0.901 for 2-8 ng/mL). These data confirmed that the standard curves of the Thio-nit method were more reproducible and the assay was more sensitive. Practically, both Thio-Nit assay and Ce-As assay were highly dependent on the rate of the reaction that was difficult and cumbersome for a large number of measurements.

A quartz crystal microbalance (QCM) method has been developed for iodide determination in food samples [19]. The method was based on a sensitive response of QCM frequency due to the mass change at piezoelectric quartz crystal electrode, after its decomposition. . The ionic iodine in the sample solution was changed to the free iodine in acidic environment and was absorbed on the gold electrode QCM where the decreased frequency was measured for estimation of iodine content in food.

A cuprite-modified carbon paste electrode was evaluated as an electrochemical sensor for iodide species in aqueous medium. The overall analysis involved the two-step procedure: the open-circuit accumulation step followed by the voltammetric quantification. In the preconcentration step, iodide was accumulated on cuprite (Cu_2O) electrode according to a surface precipitation mechanism leading to the formation of CuI . This solid was then detected either in the cathodic or in the anodic mode. The first process allows multiple successive analyses without requiring any regeneration of the electrode surface, while the anodic scan resulted in the surface oxidation of Cu_2O requiring the renewal of the electrode surface before any further accumulation experiment [20-21].

Recently, flow injection amperometric analysis with boron-doped diamond thin-film electrode has been developed for easy, rapid and high sensitivity method for determination of iodide in aqueous sample [22]. Amperometric detection was sometime problematic with adsorption of complex matrix on the working electrode surface that caused a daily ritual of disassembling the electrochemical cell and mechanically polishing the working electrode surface. Pulsed amperometric detection (PAD) with “on-line” cleaning was developed to uniform electrode and reproducible activity at the electrode.

Since the determination of iodide in water, salt, and tablet is relatively simple, while method for determination of iodide in complex matrices such as food and biological samples are quite complicated, tedious, time consuming and the results may be irreproducible. For this reason, development of the method for determination of iodide in complex matrices such as egg is challenging.

The objective of this study is to develop a simple flow injection system coupled with amperometric detection by boron-doped diamond thin film for determination of iodide in egg samples.

CHAPTER II

THEORY

2.1 Electrochemical techniques [23-24]

Electroanalytical techniques are concerned with the interplay between electricity and chemistry, namely the measurements of electrical quantities, such as current, potential, or charge, and their relationship to chemical parameters. Such use of electrical measurements for analytical purposes has found a vast range of applications, including environmental monitoring, industrial quality control, and biomedical analysis. In electrochemical systems, we are concerned with the processes and factors that affect the transport of charge across the interface between chemical phases, for example, between an electronic conductor (an electrode) and an ionic conductor (an electrolyte).

2.1.1 Cyclic voltammetry

Cyclic voltammetry is the most widely used technique for verification of qualitative information of electrochemical reactions. The great merit of cyclic voltammetry is the ability to rapidly provide considerable information on the thermodynamics of redox processes, on the kinetics of heterogeneous electron-transfer reactions, and on coupled chemical reactions or adsorption processes. Cyclic voltammetry is often the first experiment performed in an electroanalytical study. The special offer of cyclic voltammogram is a rapid location of redox potential of the electroactive species, and an easy evaluation of the effect of media upon the redox process.

Cyclic voltammetry uses a triangular potential waveform (Figure 2-1) linearly scanning the potential of a stationary working electrode and unstirred solution. Single or multiple cycles can be used upon the information sought. The resulting current from the applied potential is measured during the

potential sweep. The plot between current versus potential is termed a cyclic voltammogram.

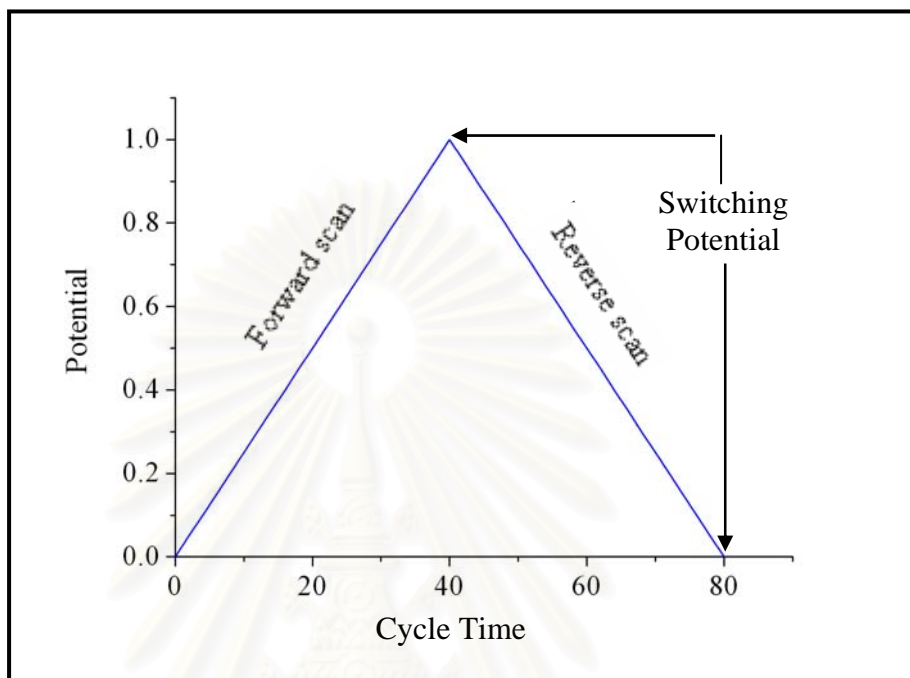


Figure 2-1 Triangular potential waveform in cyclic voltammetric experiment.

Figure 2-2 illustrates the cyclic voltammogram of a reversible redox couple during a single potential cycle. It is assumed that only the oxidized form O is present initially. Thus, the first half-cycle is scanning to a negative potential, starting from a value where no reduction occurs. Such the applied potential approaches the characteristic E° for the redox process, a cathodic current begins to increase, until a peak is reached. After traversing the potential region in which the reduction process takes place, the direction of the potential sweep is reversed. During the reverse scan, the molecules are reduced back to O and an anodic peak results.

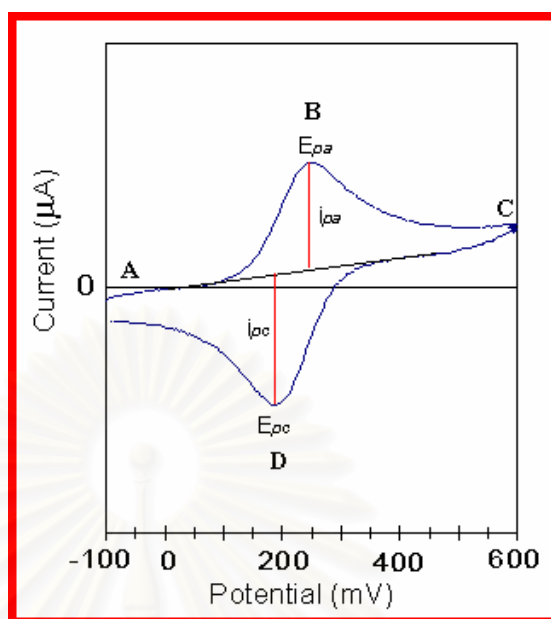


Figure 2-2 Typical cyclic voltammogram for a reversible $O + ne^- \leftrightarrow R$ redox process.

The characteristic peaks in the cyclic voltammogram are caused by the formation of the diffusion layer near the electrode surface. These can be defined by the concentration-distance profiles during the potential sweep (Figure 2-3). Figure 2-3 illustrates four concentration gradients for the reactant and product at different times corresponding to (a) the initial potential value; (b) and (d) the formal potentials during the forward and reverse scans, respectively; and (c) the achievement of a zero reactant surface concentration. Note that the continuous change in the surface concentration is coupled with an expansion of the diffusion layer thickness. Consequently, the current peaks are the continuous change of the concentration gradient with time. Hence, the increase in the peak current corresponds to the achievement of diffusion control, while the current drop exhibits a $t^{-1/2}$ dependence. For the above reasons, the reversal current has the same shape as the forward one.

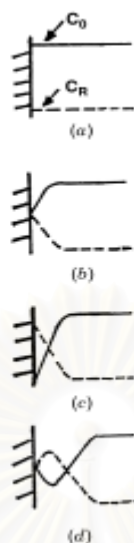


Figure 2-3 Concentration distribution of the oxidized and reduced forms of the redox couple at different times during a cyclic voltammetric experiment corresponding to (a) the initial potential; (b, d) the formal potential of the couple during the forward and reverse scans; and (c) the achievement of a zero reactant surface concentration. [24]

2.1.1.1 Data interpretation

The cyclic voltammogram is characterized by several important parameters. Four of these observables; i.e., two peak currents and two peak potentials, provide the basis for the diagnostics developed by Nicholson and Shain for analyzing the cyclic voltammetric response.

2.1.1.1.1 Reversible system

The peak current for a reversible couple (at 25°C), is given by the *Randles-Sevcik equation*:

$$i_p = (2.69 \times 10^5) n^{3/2} ACD^{1/2} v^{1/2} \quad 2.1$$

when n is the number of electrons, A is the electrode area (in cm^2), C is the concentration (in mol cm^{-3}), D is the diffusion coefficient (in $\text{cm}^2 \text{s}^{-1}$), and v is the scan rate (in V s^{-1}). Accordingly, the current is directly proportional to concentration and increases with the square root of the scan rate. The ratio of the reverse-to-forward peak currents, $i_{p,r} / i_{p,f}$, is unity for a simple reversible couple. This peak ratio can be strongly affected by chemical reactions coupled to the redox process.

The position of the peaks on the potential axis (E_p) is related to the formal potential of the redox process. The formal potential for a reversible couple is centered between $E_{p,a}$ and $E_{p,c}$:

$$E^\circ = \frac{E_{p,a} + E_{p,c}}{2} \quad 2.2$$

The separation between the peak potential (for a reversible couple) is given by

$$\Delta E_p = E_{p,a} - E_{p,c} = \frac{0.059}{n} \text{ V} \quad 2.3$$

Thus, the peak separation can be used to determine the number of electrons transferred, and as criterion for a Nernstian behavior. Accordingly, a fast one-electron process exhibits a ΔE_p of about 59 mV. Both cathodic and anodic peak potentials are independent of the scan rate. It is possible to relate the half-peak potential ($E_{p/2}$, where the current is half of the peak current) to the polarographic half-wave potential, $E_{1/2}$:

$$E_{1/2} = E_{p/2} \pm \frac{0.028}{n} \text{ V} \quad 2.4$$

(This sign is positive for a reduction process.)

2.1.1.1.2 Irreversible and Quasi-Reversible Systems

For irreversible processes, these with moving more slowly electron exchange, the individual peaks are reduced in size and widely separated (Figure 2-4, curve A). Totally irreversible systems are characterized by a shift of the peak potential with the scan rate:

$$E_p = E^\circ - \frac{RT}{\alpha n_a F} \left(0.78 - \frac{\ln k^\circ}{D^{1/2}} + \ln \left(\frac{\alpha n_a F v}{RT} \right)^{1/2} \right) \quad 2.5$$

when α is the transfer coefficient and n_a is the number of electrons involved in the charge-transfer step. Thus, E_p occurs at potentials higher than E° , with the over-potential related to k° and α . Independent of the value k° , such peak displacement can be compensated by an appropriate change of the scan rate. The peak potential and the half-peak potential (at 25°C) will differ by $48/\alpha n$ mV. Hence, the voltammogram becomes more drawn-out as αn decreases.

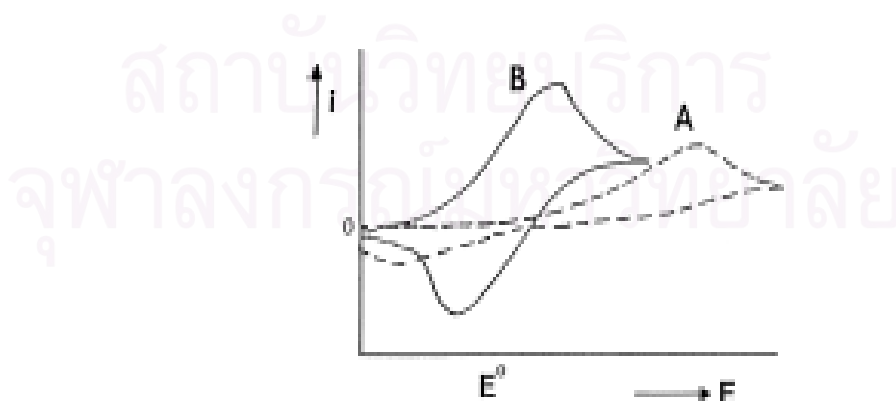


Figure 2-4 Cyclic voltammograms for irreversible (curve A) and quasi-reversible (curve B) redox processes. [24]

The peak current, given by

$$i_p = (2.69 \times 10^5)n(\alpha n_a)^{1/2} ACD^{1/2}v^{1/2} \quad 2.6$$

is still proportional to the bulk concentration, but will be lower in height (depending upon the value of α). Assuming a value of 0.5, the ratio of the reversible-to-irreversible current peak is 1.27 (i.e., the peak current for the irreversible process is about 80% of the peak for a reversible one).

For quasi-reversible systems (with $10^{-1} > k^\circ > 10^{-5} \text{ cm s}^{-1}$) the current is controlled by both the charge transfer and mass transport. The shape of the cyclic voltammogram is a function of $k^\circ/\sqrt{\pi\alpha D}$ (where $\alpha = nFv/RT$). As $k^\circ/\sqrt{\pi\alpha D}$ increases, the process approaches the reversible case. For small values of $k^\circ/\sqrt{\pi\alpha D}$ (i.e., at very fast v) the system exhibits an irreversible behavior. Overall, the voltammograms of a quasi-reversible system are more drawn-out and exhibit a large separation in peak potential compared to those of a reversible system (Figure 2-4, curve B).

2.1.1.2 Study of reaction mechanism

One of the most important applications of cyclic voltammetry is for qualitative diagnosis of chemical reactions that precede the redox process. Such reaction mechanisms are commonly classified by using the letters E and C (for the redox and chemical steps, respectively) in the order of the steps in the reaction scheme. The occurrence of such chemical reactions, which directly affect the available surface concentration of the electroactive species, is common to redox processes of many important organic and inorganic compounds. Changes in the shape of the cyclic voltammogram, resulting from the chemical competition for the electrochemical reactant or product, can be

extremely useful for elucidating these reaction pathways and for providing reliable chemical information about reactive intermediates.

For example, when the redox system is perturbed by a following chemical reaction, that is, an EC mechanism,



The cyclic voltammogram will exhibit a smaller reverse peak (because the product R is chemically removed from the surface). The peak ratio $i_{p,r}/i_{p,f}$ will thus be smaller than unity; the exact value of the peak ratio can be used to estimate the rate constant of the chemical step. In the extreme case, the chemical reaction may be so fast that all of R will be converted to Z, and no reverse peak will be observed. A classic example of such an EC mechanism is the oxidation of the drug chlorpromazine to form a radical cation that reacts with water to give an electroinactive sulfoxide. Ligand exchange reactions (e.g., of iron porphyrin complexes) occurring after electron transfer represent another example of such a mechanism.

Additional information on the rates of these (and other) coupled chemical reactions can be achieved by changing the scan rate (i.e., adjusting the experimental time scale). In particular, the scan rate controls the time spent between the switching potential and the peak potential (during which the chemical reaction occurs). Hence, as illustrate in Figure 2-5, i is the ratio of the rate constant (of the chemical step) to the scan rate, which controls the peak ratio. Most useful information is obtained when the reaction time lies within the experimental time scale. For scan rates between 0.02 and 200 V s⁻¹ (common with conventional electrodes), the accessible time scale is around 0.1-1000 ms. Ultramicroelectrodes offer the use of much faster scan rates and hence the possibility of shifting the upper limit of follow-up rate constants measurable by cyclic voltammetry. For example, highly reactive species generated by the electron transfer, and living for

25 ns can be detected using a scan rate of 10^6 V/s. A wide variety of faster reactions (including isomerization and dimerization) can thus be probed. The extraction of such information commonly requires background subtraction to correct for the large charging current contribution associated with ultrafast scan rates.

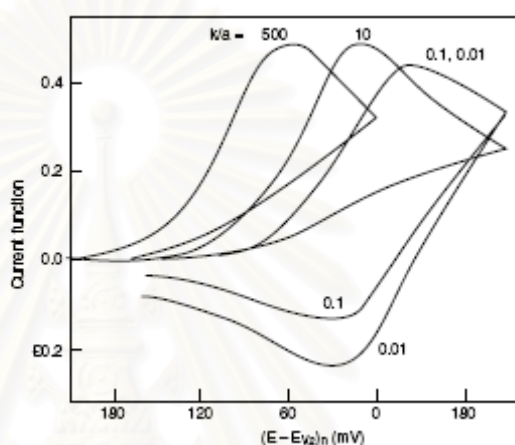


Figure 2-5 Cyclic voltammograms for a reversible electron transfer followed by an irreversible step for various ratios of chemical rate constant to scan rate, k/a , where $a = nFv/RT$. [24]

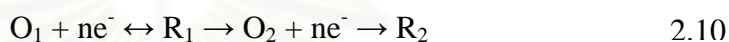
A special case of the EC mechanism is the catalytic e generation of O during the chemical step:



An example of such a catalytic EC process is the oxidation of dopamine in the presence of ascorbic acid. The dopamine quinone formed in the reduction step is reduced back to dopamine by the ascorbate ion. The peak ratio for such a catalytic reaction is always unity.

Other reaction mechanisms can be elucidated in a similar fashion. For example, for a CE mechanism, where a slow chemical reaction precedes the electron transfer, the ratio of $i_{p,r}/i_{p,f}$ is generally larger than unity, and approaches unity as the scan rate decreases. The reverse peak is usually not affected by the coupled reaction, while the forward peak is no longer proportional to the square root of the scan rate.

ECE processes, with a chemical step being interposed between electron transfer steps,



are also easily explored by cyclic voltammetry, because the two redox couples can be observed separately. The rate constant of the chemical step can thus be estimated from the relative sizes of the two cyclic voltammetric peaks.

2.1.2 Amperometry

Amperometry is an electroanalytical technique that involves the application of a constant reducing or oxidizing potential to working electrode and the subsequent measurement of the resulting steady-state current. Usually, the magnitude of the measured current is dependent on the concentration of the reduced or oxidized substance, and hence this method can be used for various analytical applications.

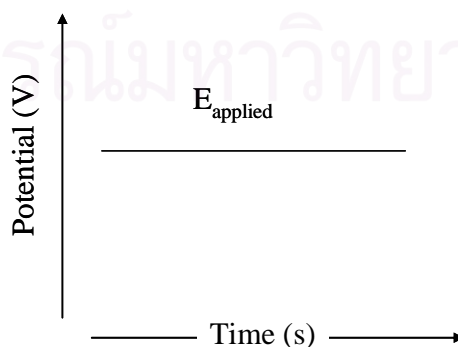


Figure 2-6 Amperometry (E-t) waveform.

2.1.3 Pulsed amperometric detection [7, 25,26]

Pulsed amperometric detection (PAD) was introduced by Johnson and LaCourse because of the problem of loss activity of noble metal electrodes associated with the fixed-potential detection of compounds such as amino acids, carbohydrates or aldehydes. Pulsed amperometric detection has more advanced the scope of liquid chromatography and electrochemistry. The most widely used PAD waveform is the three-step waveform as shown in Figure 2-7. The electrode potential is first stepped to the optimum value for detection of the electroactive species (E_{det}). After a delay time (t_{del}), during which the current mainly from double-layer charging is permitted to decay to minimal value, the analytical signal is calculated by integrating the faradaic current due to analyte oxidation for a specified time period (t_{int}). The potential then stepped to a more positive value (E_{oxd}) at which the electrode surface is oxidatively cleaned of any compounds adsorbed during the detection step. Finally, the potential is stepped to a negative value (E_{red}) to reduce the oxide layer formed at E_{oxd} , thereby regenerating the electrode activity so that the cycle may be repeated.

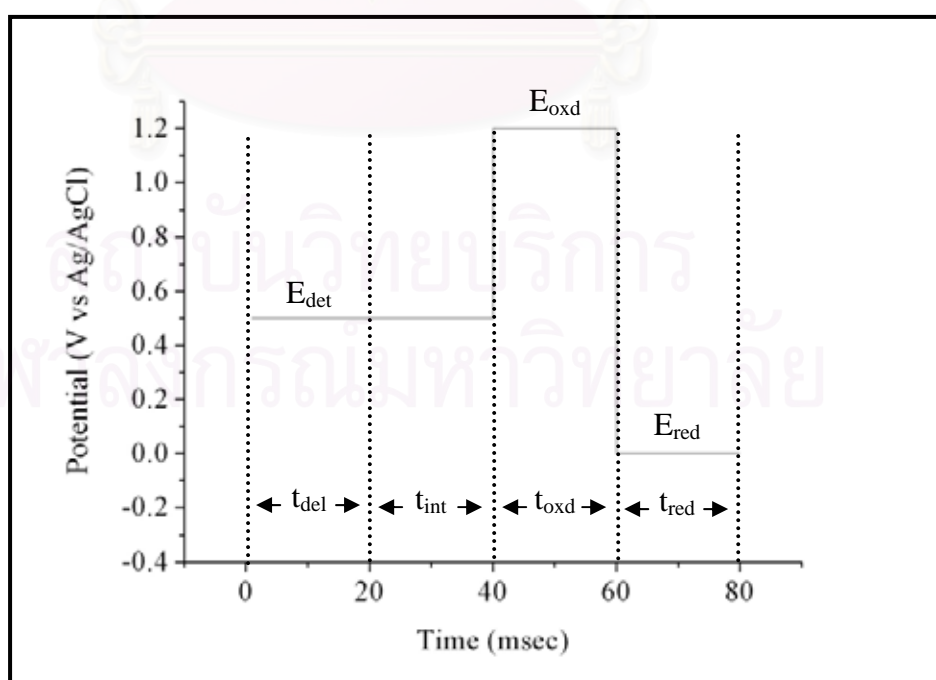


Figure 2-7 The three-step PAD waveform.

2.2 Flow injection analysis [32]

Flow injection analysis (FIA) is based on the injection of a liquid sample into a moving, non-segmented continuous carrier stream of a suitable liquid. The injection sample forms a zone, which is then transported toward a detector that continuously records absorbance, current, or other physical parameters as it continuously changes due to the passage of the sample material through the flow cell.

The simplest flow injection analyzer consists of a pump, which is used to propel the carrier stream through a narrow tube; an injection port, by means of which a well-defined volume of a sample solution is injected into the carrier stream in a reproducible manner; and a micro reactor in which the sample zone disperses and reacts with the components of the carrier stream, forming a species that is sensed by a flow through detector and recorded. A basic schematic diagram of FIA is shown in Figure 2-8.

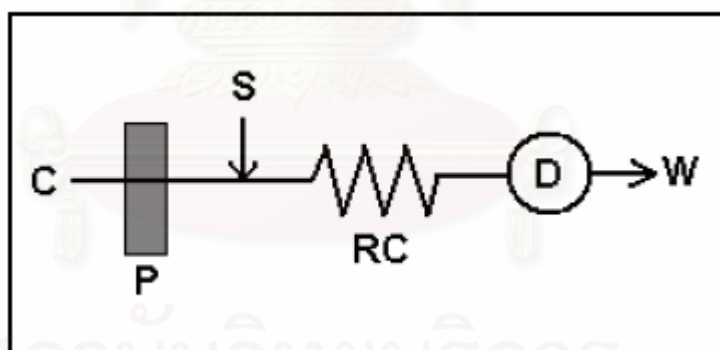


Figure 2-8 Schematic diagram of the basic FIA where C is carrier, P is pump, S is point of sample injection, RC is reaction coil, D is detector and W is waste. [32]

A typical recorder output has the form of a peak as Figure 2-9, the height (H), or area (A) of which is related to the concentration of the analyte. The time span between the sample injection (S) and the peak maximum, which yields the analytical readout as peak height H , is the residence time (T) during which the chemical reaction taking place. The well-designed FIA system has an extremely rapid response, because T is in the range of 5-20 s. Therefore, a sampling cycle is less than 30 s (roughly $T + t_b$), and thus, typically, two samples can be analyzed per minute. The injection sample volumes may be between 1 and 200 μL (typically 25 μL), which in turn requires no more than 0.5 mL of reagent per sampling cycle. This makes FIA a simple, automated microchemical technique, capable of having a high sampling rate and a minimum sample and reagent consumption.

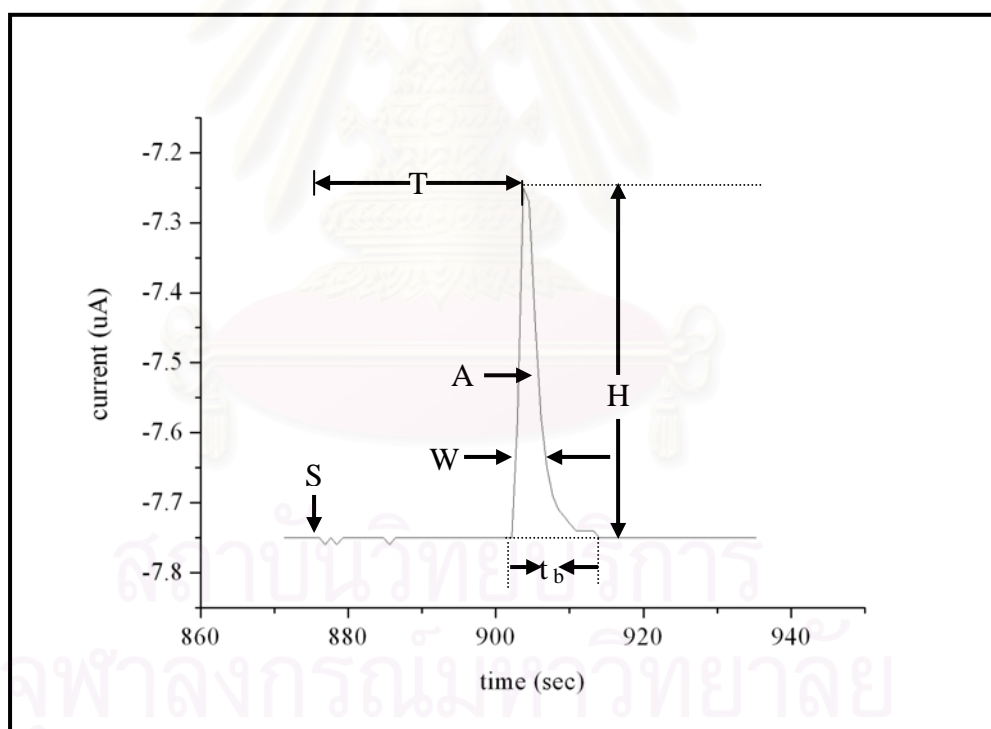


Figure 2-9 The typical output form of a peak, the recording starting at S (time of injection t_0). H is the peak height, W is the peak width at a selected level, and A is a peak area, T is the residence time corresponding to the peak height measurement, and t_b is the peak width at the baseline.

2.3 Determination of iodide in egg using catalytic colorimetric method [16, 17, 27]

The catalytic colorimetric method has been widely used for determination of iodide in food, clinical specimens and animal feeding stuffs. The reaction between iron (III) thiocyanate complex (red) and nitrite in acid can be catalyzed by iodide ion and the fade out of the complex can be detected by UV-visible at 450 nm. It is autocatalytic in nitrous acid. The reaction is often called the Sveikina reaction. An autocatalytic reaction depends on the concentration of the catalytic species. The reaction can be represented by



Alkali dry ashing is the sample preparation technique for the destruction of organic matter prior to iodide determination. It is a relatively simple method for removing the organic matters. In the open vessel the sample is placed in a suitable crucible and is dried and ashed in a muffle furnace. In this technique, recommended alkali reagent such as potassium hydroxide or potassium carbonate aids in the retention of iodide ion in the solution. These salts leave a soluble alkali iodide residue. The temperature can be varied from 400 to 600 °C and the time of ashing is from 30 min to 3 hr. The dissolved iodide ion can be separated from the insoluble residue by centrifugation.

สถาบันวิทยบริการ
จุฬาลงกรณ์มหาวิทยาลัย

CHAPTER III

EXPERIMENTAL

3.1 Instruments and Equipments

3.1.1 Electrochemical Method

1. Autolab Potentiostat (PGSTAT 30, Metrohm)
2. Rheodyne injection valve, model 7225 (Altech), with a 20 μL stainless steel injection loop (0.5 mm. i.d.)
3. Milli-Q water system, Millipore ZMQS5V00Y, (Millipore, USA)
4. Peristaltic pump (Ismatic)
5. Autopipette and tips (Gilson, Germany), 2.5, 200, 1000 and 5000 μL
6. Ag/AgCl electrode (Bioanalytical System Inc.)
7. Home-made platinum wire (Electrochemical Group, Chulalongkorn University, Thailand)
8. Glassy carbon electrode (0.07 cm^2 , Bioanalytical system Inc) pretreated by polishing with alumina powder slurries (1 and 0.05 micron, respectively) in ultrapure water on felt pads and rinsed thoroughly with ultrapure water prior to use.
9. Boron doped-diamond electrode (WD769/1, Purchased from Centre Suisse' Electronique de Microtechnique SA (CSEM) and obtained from Associate Prof. Kensuke Honda.
10. Electrolyte vessel (Metrohm, 6.1415.150)
11. Pads and alumina powder slurries of 1 and 0.05 micron, respectively. (Metrohm)
12. Thin layer flow cell (Bioanalytical System Inc.)
13. Teflon cell gasket (Bioanalytical System Inc.)
14. PEEK tubing (0.25 mm i.d.) and connecting (Upchurch)
15. Teflon tubing (1/10 inch i.d., Upchurch)

16. Cutting set (Altech)
17. Viton O-ring (0.07 cm²)
18. pH meter (Metrohm)
19. Sonicator (USA, A006651)

3.1.2 Microdialysis sampling

1. Polysulfone hollow fiber membrane with i.d. 1100 μ m, wall thickness 270 μ m and porosity 30% (Vifill 4040, ultrapure, Thailand)
2. Magnetic bar
3. Needle (0.8 x 25 mm, NIPRO)
4. Peristaltic pump (Masterflex)
5. Tubing (precision tubing, Masterflex)
6. Stirrer (Fisher scientific)

3.1.3 Catalytic colorimetric Method

1. Centrifuge (CENTAURA 2, Sanyo)
2. UV-visible spectrophotometer, HP 8453 (Hewlett Packard, USA)
3. Muffle furnace with thermostat (Carbolite, Bamford, Sheffield, UK)
4. Autopipette and tips (Eppendorf, Germany), 200 and 1000 μ L
5. Glass bottles with Teflon screw cap 500, 1000 mL (Duran)
6. Volumetric flasks 10, 25, 50, 100, 500 and 1000 mL
7. Beakers 10, 25, 50, 100, 500 and 1,000 mL
8. Porcelain crucible 10 mL
9. Conical centrifuge tube 10 mL
10. HDPE bottles with screw cap 25, 50, 125, 1000 mL (Nalgene)

3.2 Chemicals and Reagents

1. Di-sodium hydrogen orthophosphate-dihydrate (BDH)
2. Potassium carbonate (CARLO)
3. Potassium iodide (CARLO)
4. Potassium dihydrogen orthophosphate (BDH)
5. Potassium thiocyanate (CARLO)
6. Iron(III) ammonium sulfate (CARLO)
7. Zinc sulphate heptahydrate (CARLO)
8. Sodium nitrite (CARLO)
9. Nitric acid 95% (MERCK)
10. Standard buffer solution pH 4 and 7 (Metrohm)

3.3 Electrochemical Method

3.3.1 Preparation of chemical solution

3.3.1.1 Phosphate buffer as supporting electrolyte

The supporting electrolyte was prepared by weighing 8.2794 g of potassium dihydrogen phosphate, dissolving with Milli Q water, and adjusted to the required pH with 60 mM di-sodium hydrogen phosphate, prepared by dissolving 0.5340 g of di-sodium hydrogen phosphate and diluting in 50 mL of Milli Q water.

3.3.1.2 Stock Standard Iodide Solutions

The stock standard iodide solution of 1000 mg/L was prepared by dissolving 32.7 mg of potassium iodide in supporting electrolyte and diluting the solution in a 25 mL volumetric flask.

3.3.1.3 Working Standard Iodide Solution

The standard iodide solution of 2 mg/L was prepared daily by pipetting 50 μL of the stock standard iodide solution and adjusted to 25 mL with electrolyte solution. Working standard iodide solutions were prepared by diluting the standard iodide solutions of 2 mg/mL with electrolyte solution.

3.3.2 Cyclic voltammetric study

The cyclic voltammetry provides qualitative information of iodide about electrochemical reactions. The electrochemical measurements were performed in a single compartment glass cell using a potentiostat. Figure 3-1 showed the electrochemical cell for cyclic voltammetric experiment. A Ag/AgCl electrode was used as a reference electrode and a platinum wire was employed as an auxiliary electrode. The boron-doped diamond electrode (0.07 cm^2) was used as working electrode. The working electrode (boron doped diamond or glassy carbon) was pressed against a smooth ground joint at the bottom of the cell isolated by O-ring (area 0.07 cm^2).



Figure 3-1 The electrochemical cell for cyclic voltammetric study.

3.3.3 Background current [22]

The background current is composed of contribution due to double-layer charging process (known as charging current) and redox reactions of impurities such as the solvent, supporting electrolyte, or electrode. Within the working potential range, the charging current is the major component of the background which defines the detection limit. Thus, the background current was studied. The background current of boron-doped diamond electrode was compared to that of glassy carbon electrode. The experiment was carried out in 60 mM phosphate buffer (pH 5) at the scan rate of 50 mV/s.

3.3.4 pH optimization

This experiment was studied for the appropriate pH for reaction of iodide. The study was performed using 63.5 mg/L iodide solutions prepared in phosphate buffer pH 3, 4, 5, 6, 7, 8 and 9 at the scan rate of 50 mV/s.

3.3.5 Effect of scan rate

This experiment was studied for the behavior of iodide at the electrode surface. Experiments were performed using 63.5 mg/L iodide solutions at various scan rates of 10, 20, 25, 50, 75, 100, 200, 300, 400 and 500 mV/s.

3.3.6 The flow injection analysis with amperometric detection using boron-doped diamond electrode

3.3.6.1 Hydrodynamic voltammetry

Hydrodynamic voltammetry was performed to find the optimum potential of iodide for the flow injection analysis with amperometric determination. The data are obtained by recording the background current and the peak current of four injections of 20 μ l of 100 mg/L

iodide solution at each potential such as 0.3, 0.4, 0.5, 0.6, 0.7, 0.8, 0.9, 1.0, 1.1, 1.2 V. The ratios of peak current and background current are plotted as a function of applied potential. The maximum peak current to background current ratio would be the optimum potential of iodide for the flow injection with amperometric determination.

3.3.6.2 Amperometric detection

Amperometric detection coupled flow injection (FI) system was used for determination of iodide. Figure 3-2 shows the FI manifold [22] with amperometric detection using boron-doped diamond as working electrode. The flow injection analysis system used in this experiment consisted of a thin layer flow cell, an injection port with a 20 μL injection loop, a reagent delivery module or a peristaltic pump and an electrochemical detector. The mobile phase was regulated by the peristaltic pump at 1 mL/min. Figure 3-3 shows the thin layer flow cell for the flow injection system, which consisted of a silicon rubber gasket as a spacer, a Ag/AgCl electrode as a reference electrode, a stainless steel outlet tube as an auxiliary electrode, and the boron-doped diamond pressed at the outlet of the flow cell as working electrode. The experiments were performed in a copper Faradaic cage to reduce electric noise.

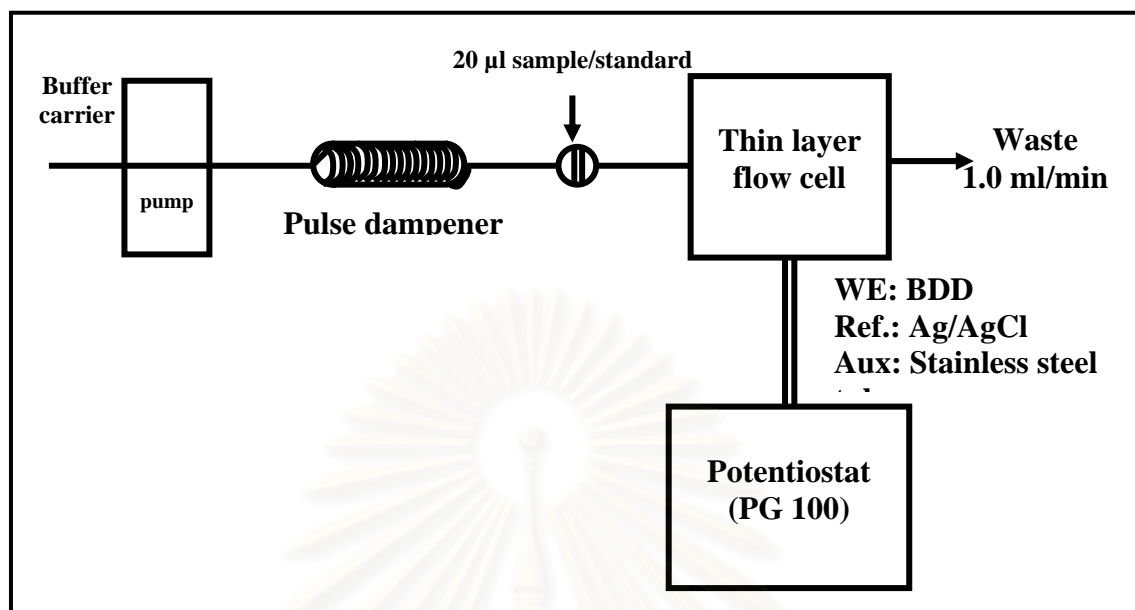


Figure 3-2 The FI manifold with amperometric detection using BDD as a working electrode and 60 mM phosphate buffer at pH 5 as carrier. [22]

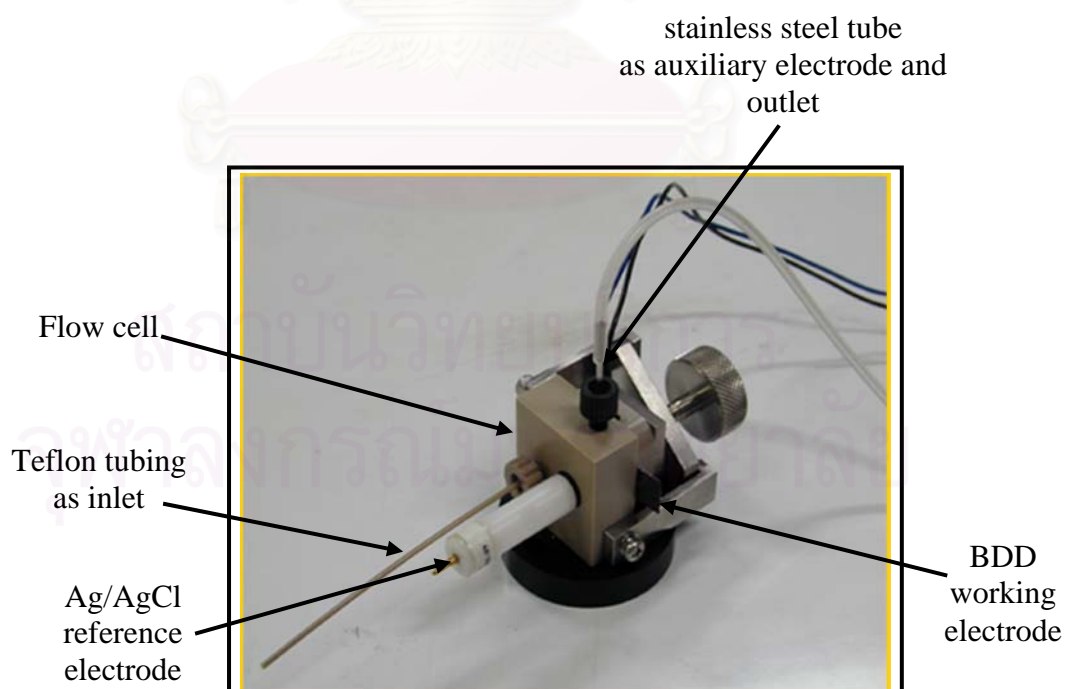


Figure 3-3 The thin layer flow cell for the flow injection with amperometry

3.3.6.3 Calibration and linearity for flow injection analysis with amperometric detection using boron-doped diamond electrode

Each concentration of standard solutions at 20, 30, 40, 50, 60, 70, 80, 90, and 100 mg/L was injected in duplicate. The calibration curves were plotted between the peak heights and the concentrations. Linear regression method was used to obtain slope, intercept and R^2 .

3.3.6.4 Limit of detection (LOD) and limit of quantitation (LOQ) for flow injection analysis with amperometric detection using boron-doped diamond electrode

The limit of detection (LOD) was defined as the concentration giving a signal of $Y_B + 3S_B$, where Y_B was blank signal and S_B was standard deviation of blank signal. The corresponding concentration was then calculated from the calibration equation. The limit of quantitation (LOQ) was the concentration giving a signal of $Y_B + 10S_B$.

3.3.6.5 Precision and Accuracy for flow injection analysis with amperometric detection using boron-doped diamond electrode

The accuracy and precision of the method were evaluated by determination of recovery and relative standard deviation of the repeat analysis of iodide solution. The measurements were done in triplicate.

3.3.7 The flow injection analysis with pulsed amperometric detection (FI-PAD) using boron-doped diamond electrode

3.3.7.1 Pulsed amperometric detection (PAD)

Pulsed amperometric detection was used to lowering the detection limit and cleaning the electrode surface with flow injection analysis. The FI manifold and other conditions were similar to flow injection analysis with amperometric detection except the potential waveform.

3.3.7.2 PAD waveform optimization

The PAD waveform parameters were optimized through a series of injection of 100 mg/L standard iodide solution in the flow injection system by varying parameters as in Table 3-1. The signal-to-background ratios were plotted versus the varied parameter to obtain the optimal values.

Table 3-1 The varied parameters for PAD optimization

Parameter	Studied range
1. Detection step	
E_{det} (V vs. Ag/AgCl)	0.3 - 1.2
t_{del} (msec)	30 – 1000
t_{int} (msec)	30 - 700
2. Oxidation step	
E_{oxd} (V vs. Ag/AgCl)	0.9 - 1.2
t_{oxd} (msec)	500 - 900
3. Reduction step	
E_{red} (V vs. Ag/AgCl)	0.3 - 1.1
t_{red} (msec)	30 - 300

3.3.7.3 Calibration and linearity for FI-PAD with boron-doped diamond electrode

Each concentration of standard solutions at 20, 50, 100, 200, 500, 800, 1000, 2000, 3000, 4000 and 5000 $\mu\text{g/L}$ was injected in duplicate. The calibration curves were plotted between the peak heights and the concentrations. Linear regression method was used to obtain slope, intercept and R^2 .

3.3.7.4 Limit of detection (LOD) and limit of quantitation (LOQ) for FI-PAD with boron-doped diamond electrode

The limit of detection (LOD) was defined as the concentration giving a signal of $Y_B + 3S_B$, where Y_B was blank signal and S_B was standard deviation of blank signal. The corresponding concentration was then calculated from the calibration equation. The limit of quantitation (LOQ) was defined as the concentration giving a signal of $Y_B + 10S_B$.

3.3.7.5 Precision and Accuracy for FI-PAD with boron-doped diamond electrode

The accuracy and precision of the method were evaluated by determination of recovery and relative standard deviation of the repeat analysis of iodide solution. The measurements were done in triplicate.

3.4 Colorimetric Method [16-17]

3.4.1 Preparation of chemical solutions

3.4.1.2 Stock Standard Iodide Solution

The stock standard iodide solution of 1000 mg/L was prepared by dissolving 32.7 mg of potassium iodide in Milli Q water and diluting the solution in a 25 mL volumetric flask.

3.4.1.2 Working Standard Iodide Solutions

The standard iodide solution of 2 mg/L was prepared daily by pipetting 50 μ L of the stock standard iodide solution adjusted to 25 mL with Milli Q water. Working standard iodide solutions were prepared by diluting the standard iodide solutions of 2 mg/mL with Milli Q water.

3.4.1.3 Potassium carbonate solution 30% (m/V)

A 30 g of potassium carbonate (K_2CO_3) was dissolved in Milli Q water and diluted to 100 mL in a volumetric flask.

3.4.1.4 Potassium thiocyanate solution 0.023% (m/V)

A 0.23 g of potassium thiocyanate (KSCN) was dissolved in Milli Q water and diluted to 1.0 L in a volumetric flask.

3.4.1.5 Sodium nitrite solution 2.07% (m/V)

Sodium nitrite ($NaNO_2$) solution was freshly prepared by dissolving 2.07 g $NaNO_2$ in Milli Q water and diluted to 100 mL in a volumetric flask.

3.4.1.6 Ammonium iron(III) sulphate reagent

A 77 g of ammonium iron(III) sulphate [$\text{NH}_4\text{Fe}(\text{SO}_4)_2 \cdot 12\text{H}_2\text{O}$] was dissolved in approximately 400 mL of Milli Q water and a 167 mL of concentrated nitric acid (65%) was added and diluted to 1.0 L in a volumetric flask.

3.4.1.7 Zinc sulphate solution 10% (m/V)

A 10 g of zinc sulphate ($\text{ZnSO}_4 \cdot 7\text{H}_2\text{O}$) was dissolved in Milli Q water and diluted to 100 mL in a volumetric flask.

3.4.2 Alkali Dry Ashing

Alkali dry ashing is a sample preparation process typically for food and biological samples. Generally the sample is dried and ashed with high temperature furnace. Into a clean, dry crucible, approximately 0.5 g of homogenized egg sample was accurately weighted, 0.5 mL of potassium carbonate and 0.25 mL of zinc sulfate solution was added. The slurry was stirred and dried on a hotplate at level 6 for 45 min or until no smoke. The crucible was then covered with a lid and placed in a muffle furnace at 550°C for 2 hr. Another 1 mL of zinc sulfate solution was added after it was cooled to room temperature. The drying and ashing processes were repeated. The cooled ash, normally white or gray in color, was transferred to a centrifuge tube with 25 mL of Milli Q water, and centrifuged for 10 min. The sample solution was decanted and stored in a clean HDPE bottle.

3.4.3 Catalytic colorimetric method

A 4 mL of standard iodide solution or sample solution was pipetted into centrifuge tube. Then, 1 mL of 0.023% (m/V) potassium thiocyanate solution, 2 mL of ammonium iron (III) sulphate in nitric acid and 1 mL of milli Q water were added, successively. Then, a 1 mL of NaNO_2 was added to the solution. The solution was shaken and waited for 15 min. The absorbance of the fading color was measured by the UV-VIS spectrophotometer at 450 nm. A series of the solution could be prepared in the same way. A 1 mL of NaNO_2 was added to each solution for every 2 min interval and each solution was measured for the absorbance every 15 min.

3.4.4 Calibration and linearity for catalytic colorimetric method

The standard iodide solutions of 4, 8, 12, 16 and 20 $\mu\text{g/L}$ were used for calibration. The measurement was done in duplicate. The calibration curves were plotted between the absorbance and the concentrations. The linear regression method was used to obtain slope, intercept and R^2 .

3.4.5 Limit of Detection (LOD) and Limit of Quantitation (LOQ) for catalytic colorimetric method

The limit of detection (LOD) was defined as the concentration giving a signal of $Y_B + 3S_B$, where Y_B was blank signal and S_B was standard deviation of blank signal. The corresponding concentration was then calculated from the calibration equation. The limit of quantitation (LOQ) was defined as the concentration giving a signal of $Y_B + 10S_B$.

3.4.6 Precision and Accuracy for catalytic colorimetric method

The accuracy and precision of the method were evaluated by determination of recovery and relative standard deviation of the repeat analysis of iodide solution. The measurements were done in triplicate.

3.5 Application of the methods for determination of iodide in egg samples

Egg samples were purchased from a local market. The whole egg including its shell was weighed but only egg was used. The eggs were homogenized prior to use. The experiments were conducted in batches. Each batch was consisted of a number of certain weights of homogenized egg samples. The samples were divided into two batches for determination of iodide by electrochemical method and by catalytic colorimetric method. The results were compared.

CHAPTER IV

RESULTS AND DISCUSSION

4.1 Electrochemical method

4.1.1 Cyclic voltammetric study

4.1.1.1 Background current

In this experiment, the 60 mM phosphate buffer pH 5 was used as supporting electrolyte employed to eliminate electromigration effects and maintain a constant ionic strength. The background current flow in absence of the electroactive species of interest was composed of contributions due to double-layer charging process that limited the working potential range and limit of detection [24]. Therefore, the preliminary work focused on a comparison of the background currents that obtained with boron-doped diamond (BDD) electrode and glassy carbon (GC) electrode. Figure 4-1 showed the overlaid background voltammograms of 60 mM phosphate buffer (pH 5) at BDD electrode and GC electrode, which were obtained from batch experiment. The respective background current for the GC electrode was higher than that obtained from boron-doped diamond electrodes. There were three possibilities that could explain the low background current [28]. The first assumption was the relative absence of electroactive carbon-oxygen functionalities on the hydrogen terminated diamond surface as compared with glassy carbon but this assumption explained only some, but not all, of the low current for BDD electrode. The second contributing factor might be the lower charge carrier concentration due to the semimetal-semiconductor nature of BDD electrode. A lower state at given potential, or lower charge carrier concentration, would lead to reduced accumulation of counterbalancing ions and water dipoles on the solution side of the interface, thereby lowering the background current. The third possible contributing factor could be that the diamond surface was constructed like an array of microelectrodes. In other words, perhaps the

diamond surface had “electrochemically active” sites alternatively separated by less reactive or more insulating regions.

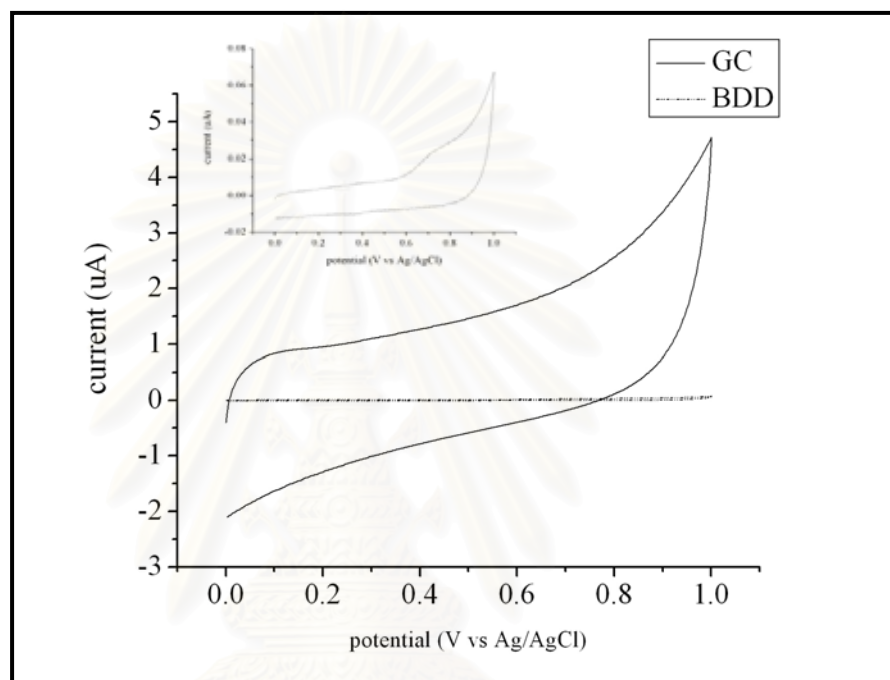


Figure 4-1 The overlaid background voltammograms of 60 mM phosphate buffer (pH 5) at BDD electrode (dotted line) and at GC electrode (solid line). The scan rate was 50 mV/s. The inserting figure show the background current at BDD electrode on a large scale.

สถาบันวิทยบริการ
จุฬาลงกรณ์มหาวิทยาลัย

There were some reports of cyclic voltammograms of iodide on platinum, gold, and glassy carbon electrode suggesting that the oxidation sequence of iodide at the working electrodes [22] can be represented by the following reactions:



Figure 4-2 and 4-3 illustrated the cyclic voltammograms of 63.5 mg/L iodide in 60 mM phosphate buffer (pH 5) at BDD electrode and GC electrode, respectively. The BDD electrode exhibited well-defined quasi-reversible oxidation peaks at 0.57 and 0.79 V versus Ag/AgCl and GC electrode provided the oxidation peaks at 0.48 and 0.74 V versus Ag/AgCl. The first oxidation peak current, subtracted from background current was 8.58 μA at BDD electrode and was 7.86 μA at GC electrode. Therefore, it was expected that BDD electrode would provide a better sensitivity. For our work, we employed only the first oxidation peak current.

4.1.1.2 Optimal pH

The buffer pH was studied for appropriate electrochemical reaction of iodide. Buffer pH was investigated from pH 3 to 8 and the voltammogram were shown in Figure 4-4 and 4-5. The BDD electrode and GC electrode exhibited well-defined cyclic voltammograms of iodide in all pH. It was observed that the oxidation peak currents slightly shift to positive potentials and background current was increased with the higher pH. In addition, the hydrogen terminal on BDD electrode might be anodized to oxygen terminal in the more acidic solution that caused an adsorption of product or complex matrix on the electrode surface. For these reasons, pH 5 was chosen as the optimal pH for further studies at the BDD electrode.

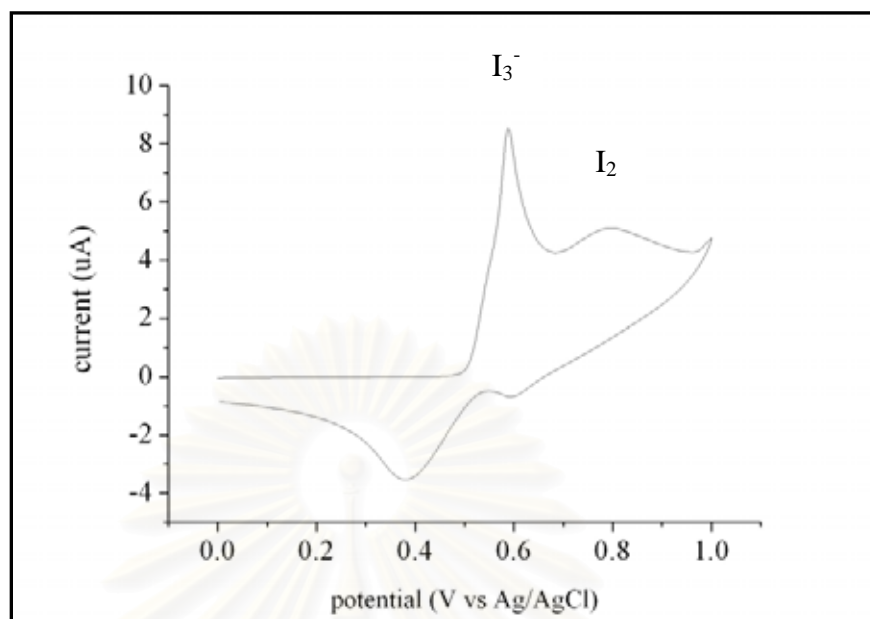


Figure 4-2 The cyclic voltammogram of 63.5 mg/L iodide in 60 mM phosphate buffer (pH 5) at BDD electrode. The scan rate was 50 mV/s.

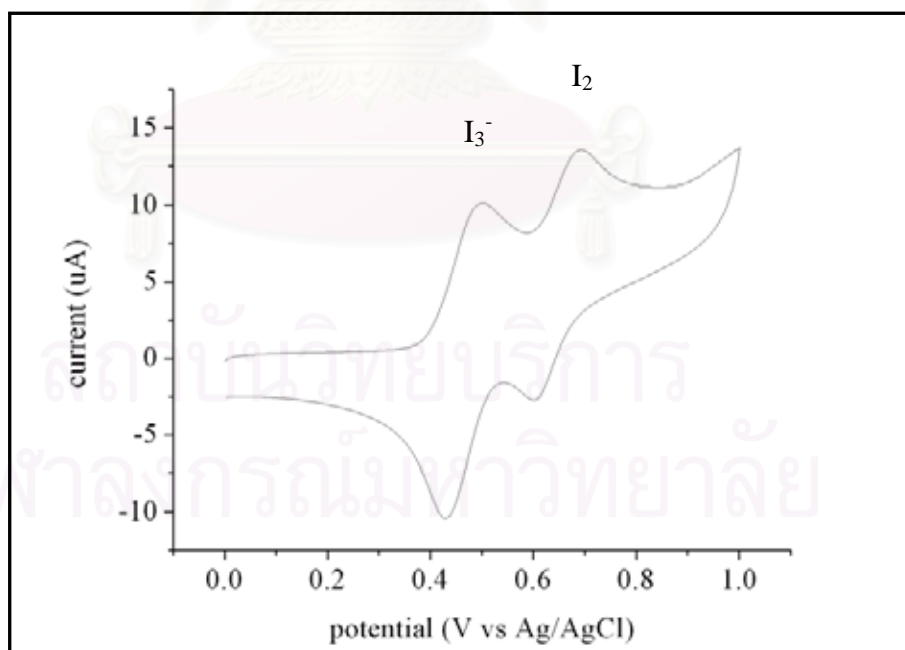


Figure 4-3 The cyclic voltammogram of 63.5 mg/L iodide in 60 mM phosphate buffer (pH 5) at GC electrode. The scan rate was 50 mV/s.

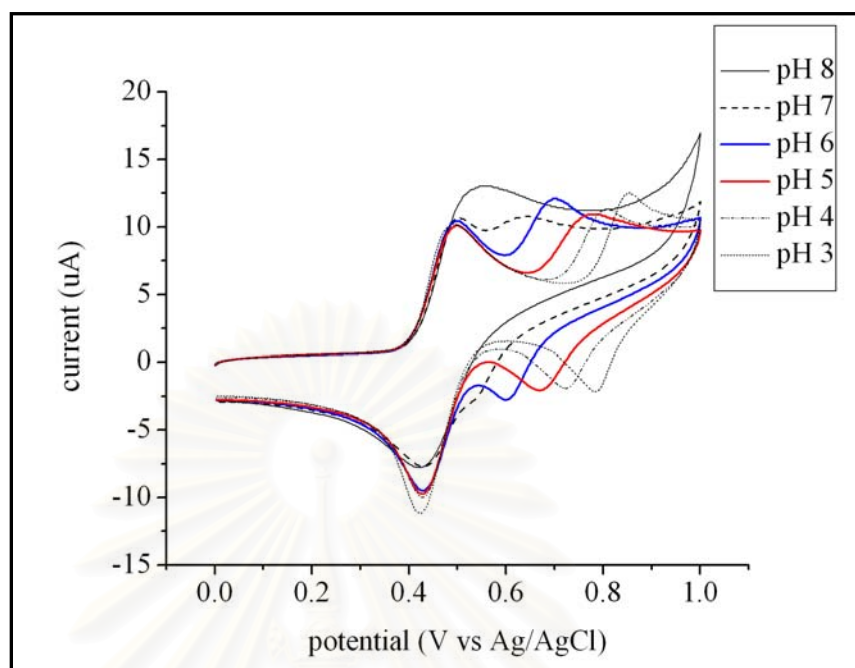


Figure 4-4 Overlaid cyclic voltammograms of 63.5 mg/L iodide at BDD electrode in 60 mM phosphate buffer pH 3 to pH 8.

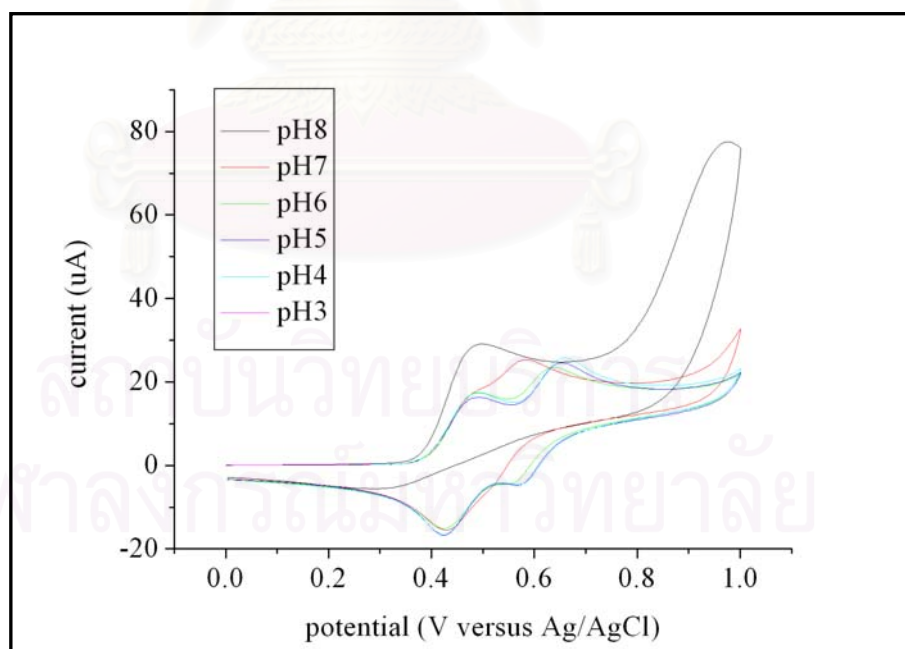


Figure 4-5 Overlaid cyclic voltammograms of 63.5 mg/L iodide at GC electrode in 60 mM phosphate buffer pH 3 to pH 8.

4.1.1.3 Effect of scan rate

The effect of the scan rate on the electrochemical behaviors of iodide was investigated at 10, 25, 50, 75, 100, 200, 300, 400 and 500 mV/s. The current responses of iodide at different scan rate and the relationship between the current responses and the square root of the scan rate for iodide at BDD electrode and GC electrode were illustrated in Figures 4-6 to 4-9, respectively. From these results, the current response of iodide was directly proportional to the square root of the scan rate. It can be concluded that the diffusion process controlled the transportation of these analytes from the bulk solution to the electrode surface [24]. From the cyclic voltammograms displayed in these figures, the oxidation of these selected analytes underwent the irreversible reaction

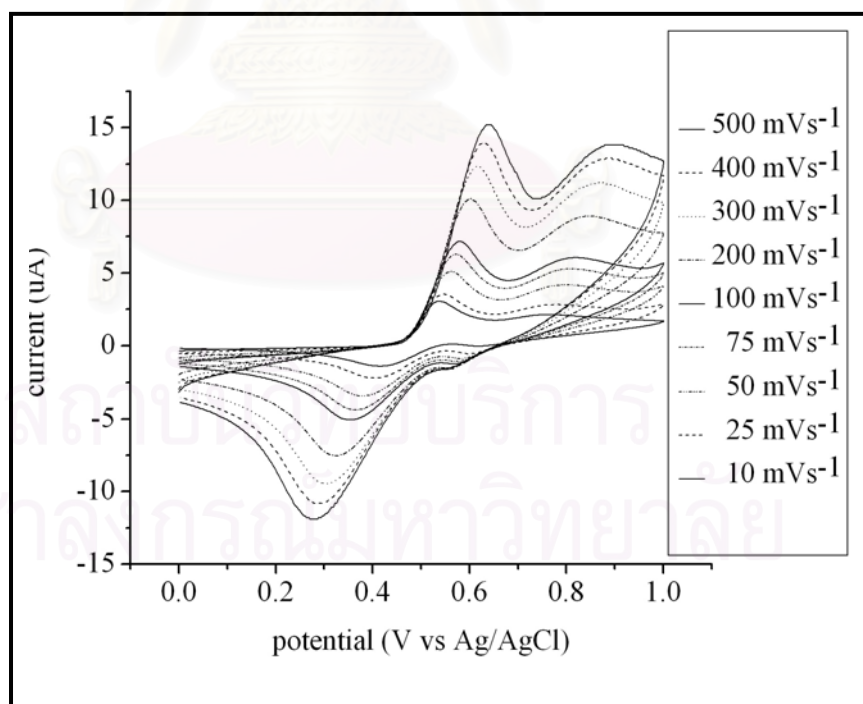


Figure 4-6 Cyclic voltammograms of 63.5 mg/L iodide in phosphate buffer (pH 5) at BDD electrode for various scan rates.

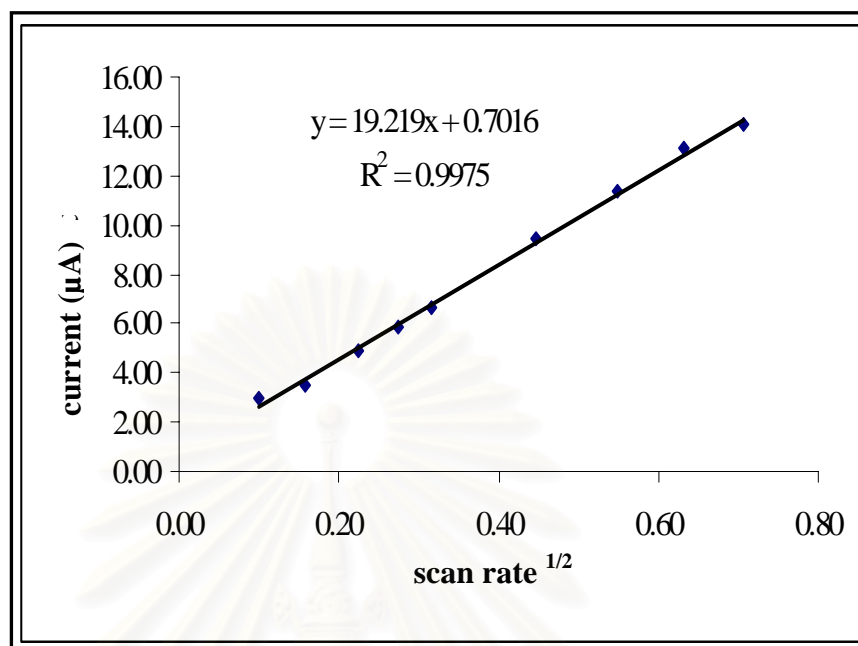


Figure 4-7 The relationship between the oxidation current and the square root of the scan rates at BDD electrode.

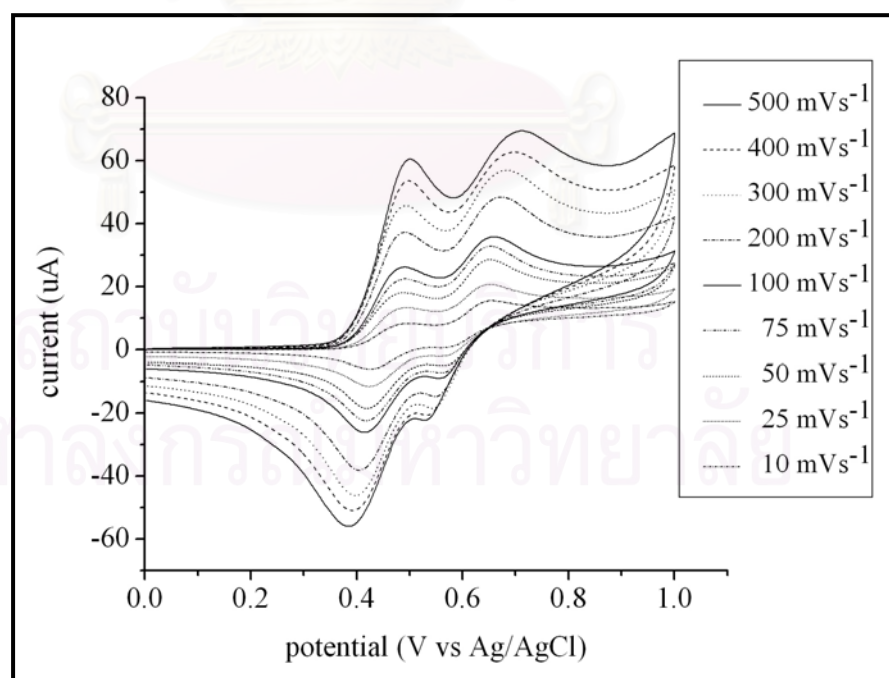


Figure 4-8 Cyclic voltammogram of 63.5 mg/L iodide in phosphate buffer (pH 5) at GC electrode for various scan rates.

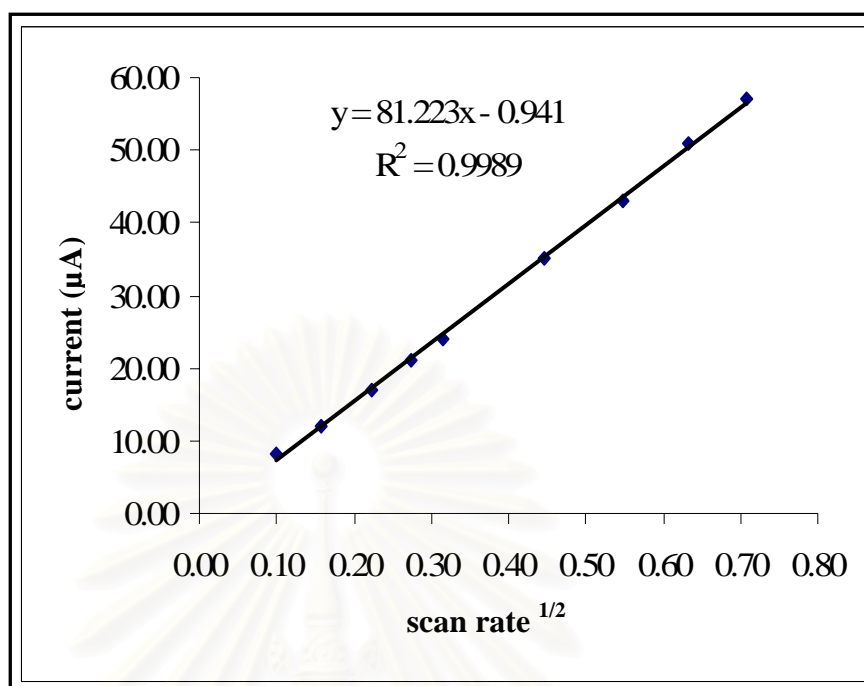


Figure 4-9 The relationship between the oxidation current and the square root of the scan rates at GC electrode.

4.1.2 Flow injection analysis with amperometric detection using boron-doped diamond electrode

4.1.2.1 Hydrodynamic Voltammetry

This part was carried out using a flow injection system. Figure 3-3 showed the most sensitive oxidation potential for determination of iodide by flow injection analysis with amperometric detection. Figure 4-10 showed the hydrodynamic voltammogram obtained at the BDD electrode for 20 µL injection of 100 mg/L iodide in 60 mM phosphate buffer (pH 5) at various potentials. The average current of the four injections and background current of each data were shown in figure 4-11. The signal-to-background ratio (S/B) was calculated and the results were presented in Figure 4-12. According to the results, the maximum S/B ratio was observed at 0.8 V. This potential was near to the peak

potential observed in the corresponding cyclic voltammogram at the same concentration. Hence, this potential was used for the amperometric detection with flow injection analysis experiments.

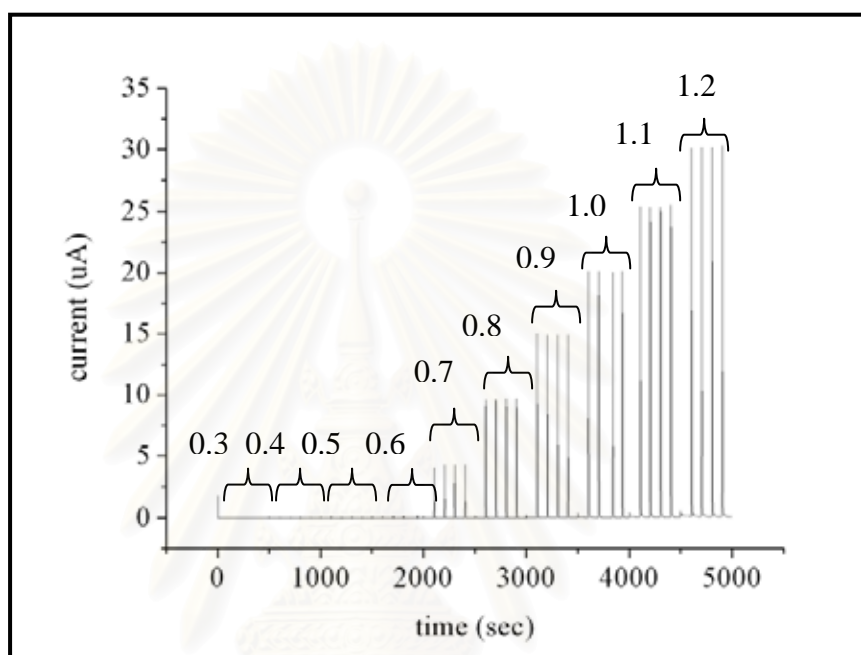


Figure 4-10 Hydrodynamic voltammograms for FI-amperometry with BDD electrode of 100 mg/L iodide in 60 mM phosphate buffer (pH 5) at various potentials.

สถาบันวิทยบริการ
จุฬาลงกรณ์มหาวิทยาลัย

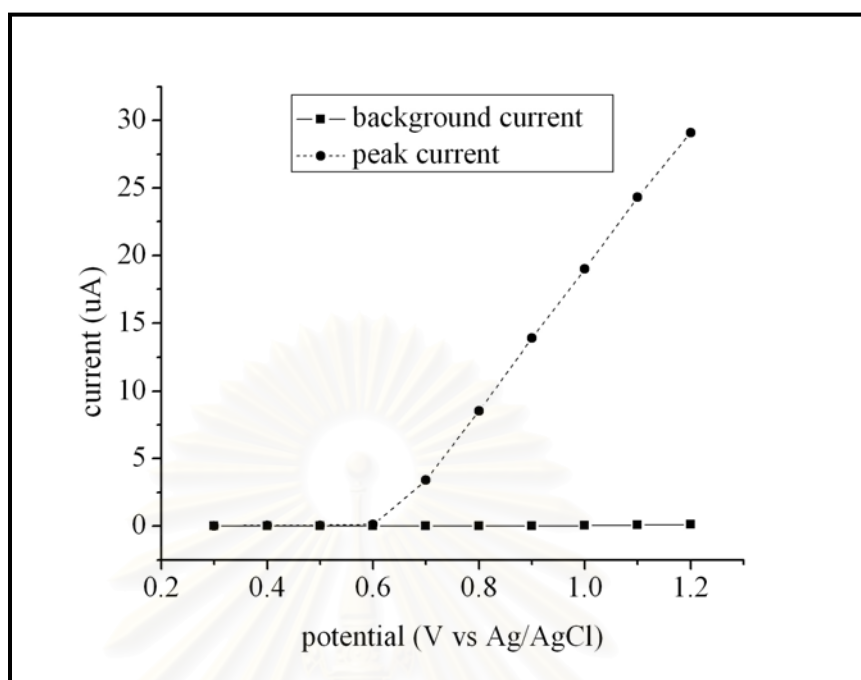


Figure 4-11 Average hydrodynamic signals for FI-amperometry with BDD electrode of background currents, 60 mM phosphate buffer (pH 5) and peak currents of 100 mg/L iodide at various potentials.

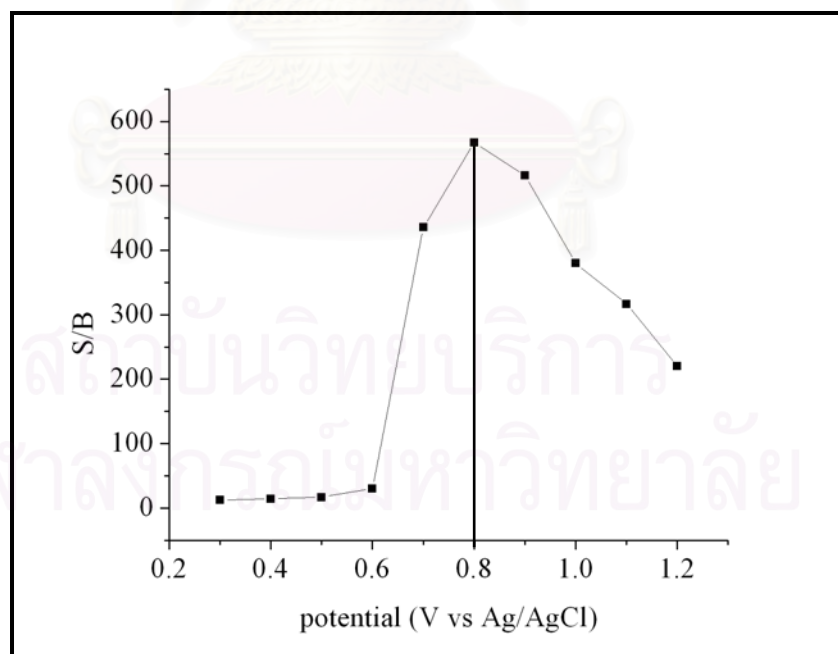


Figure 4-12 Plot of the signal-to-background ratio (S/B) for FI-amperometry with BDD electrode of 100 mg/L iodide in 60 mM phosphate buffer (pH 5) at various potentials

4.1.2.2 Method evaluation for flow injection analysis with amperometric detection using boron-doped diamond electrode

The method linearity between the current responses of iodide and iodide concentrations ranging from 30 to 100 mg/L was studied. Figure 4-13 showed the plot of the height of peak currents versus iodide concentrations. A linear dynamic range of 30 to 100 mg/g was observed correlation coefficient, $R^2 = 0.9974$. The limit of detection of 11.8 mg/L and the limit of quantitation of 28.4 mg/L were determined from 6 replicate injections of reagent blank. The recovery was 91% with 9%RSD (N=3) using 500 $\mu\text{g/L}$ standard iodide solution.

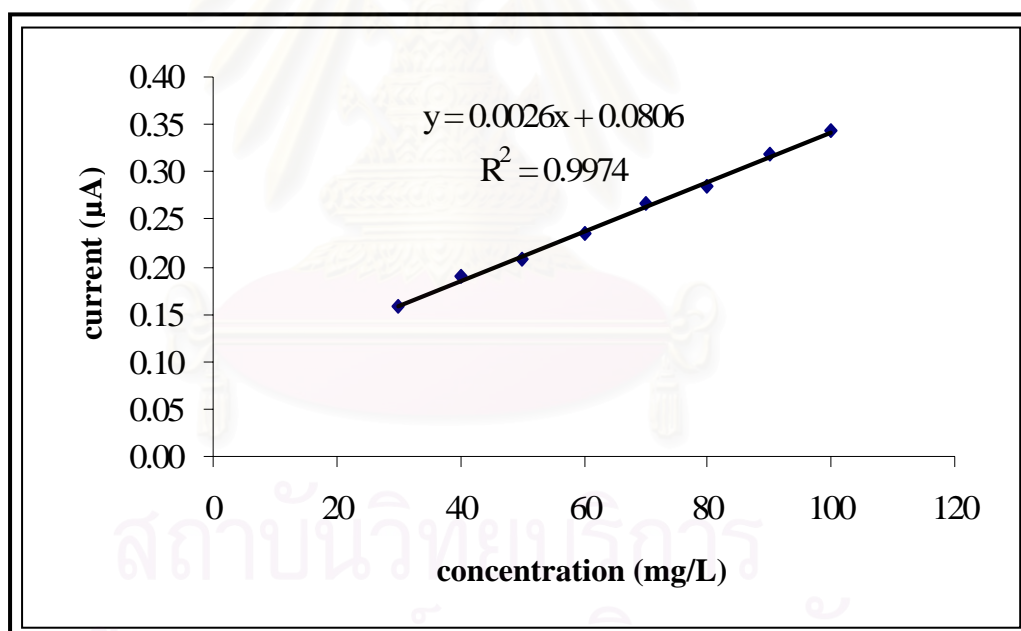


Figure 4-13 Linear dynamic range of iodide determined by flow injection analysis with amperometric detection with boron-doped diamond electrode.

4.1.3 Flow injection analysis with pulsed amperometric detection using boron-doped diamond electrode (FI-PAD-BDD)

4.1.3.1 Optimal PAD

The PAD waveform parameters such as detection potential (E_{det}), delay time (t_{del}), integration time (t_{int}), oxidation potential (E_{oxd}), oxidation time (t_{oxd}), reduction potential (E_{red}), and reduction time (t_{red}) were optimized one factor at a time using 100 mg/L iodide standard solution. The potential range used for optimization of E_{det} was chosen from the potential region in the hydrodynamic voltammogram (Figure 4.10), where the oxidation of iodide occurred. The detection potential (E_{det}) was varied from +0.3 to +1.2 V versus Ag/AgCl at the boron-doped diamond electrode. The signal to noise ratio were obtained for each potential and the result was shown in Figure 4-12. Then the delay time (t_{del}) was varied from 30 to 1000 msec. The detection potential (E_{det}), integration time (t_{int}), oxidation potential (E_{oxd}), oxidation time (t_{oxd}), reduction potential (E_{red}) and reduction time (t_{red}) were kept constant at 0.8 V, 200 msec, 1.2 V, 200 msec, 0.3 V and 200 msec, respectively. The signal to noise ratio were obtained and the result was shown in Figure 4-14. After that the integration time (t_{int}) was varied from 30 to 700 msec. The detection potential (E_{det}), delay time (t_{del}), oxidation potential (E_{oxd}), oxidation time (t_{oxd}), reduction potential (E_{red}) and reduction time (t_{red}) were kept constant at 0.8 V, 30 msec, 1.2 V, 200 msec, 0.3 V and 200 msec, respectively. The signal to noise ratio were obtained and the result was shown in Figure 4-15.

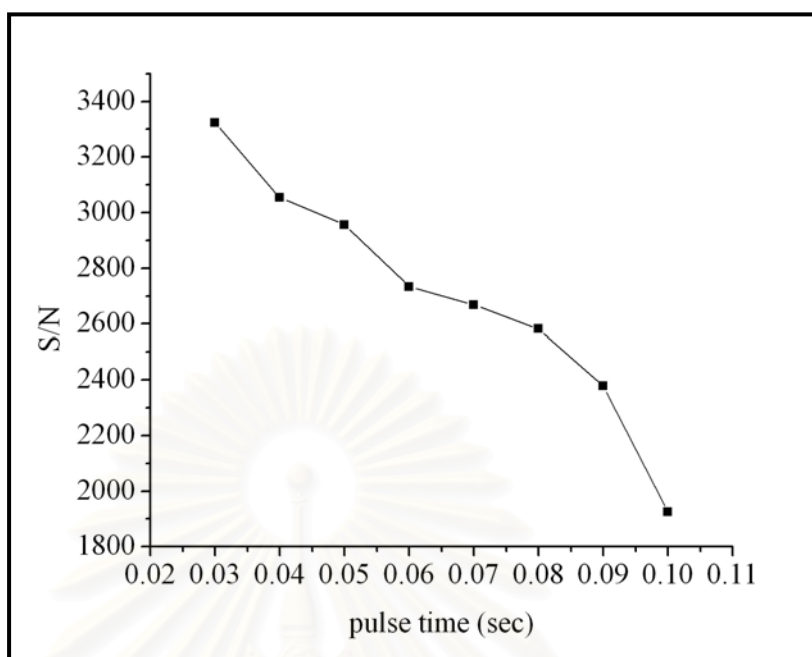


Figure 4-14 FI-PAD-BDD response as a function of t_{del} for 100 mg/L of iodide at the boron-doped diamond electrode.

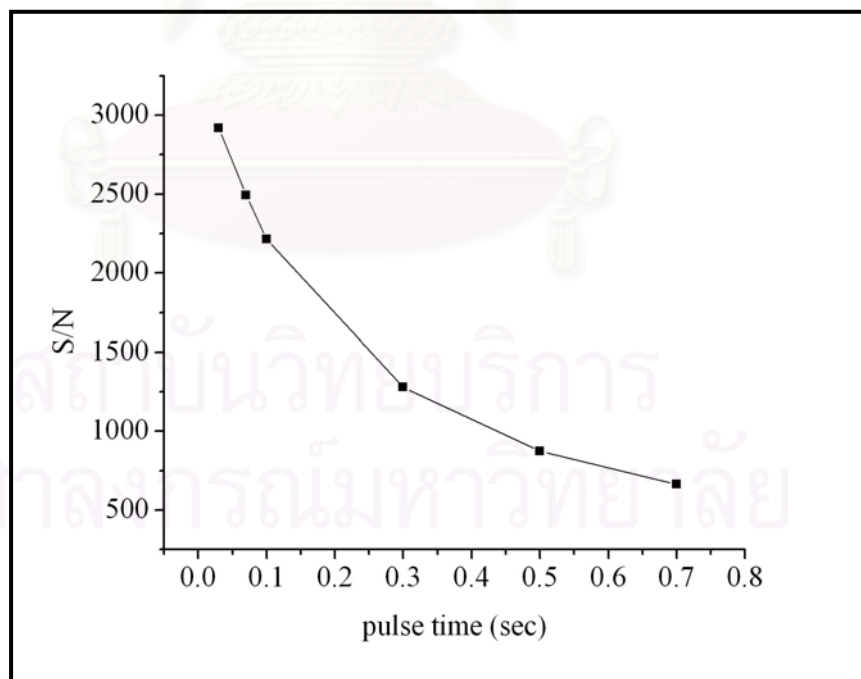


Figure 4-15 FI-PAD-BDD response as a function of t_{int} for 100 mg/L of iodide at the boron-doped diamond electrode.

To receive reproducible signals, the electrode should be pulsed adequately more positive potential to remove adsorbed species [25]. The oxidation potential (E_{oxd}) was varied from +0.9 to +1.2 V versus Ag/AgCl at the boron-doped diamond electrode. The detection potential (E_{det}), delay time (t_{del}), integration time (t_{int}), oxidation time (t_{oxd}), reduction potential (E_{red}) and reduction time (t_{red}) were kept constant at 0.8 V, 30 msec, 30 msec, 200 msec, 0.3 V and 200 msec, respectively. The signal to noise ratio were obtained and the result was shown in Figure 4-16. The variation of oxidation time (t_{oxd}) was optimized from 500 to 900 msec. The detection potential (E_{det}), delay time (t_{del}), integration time (t_{int}), oxidation potential (E_{oxd}), reduction potential (E_{red}) and reduction time (t_{red}) were kept constant at 0.8 V, 30 msec, 30 msec, 1.2 V, 0.3 V and 200 msec, respectively. The signal to noise ratio were obtained and the result was shown in Figure 4-17.

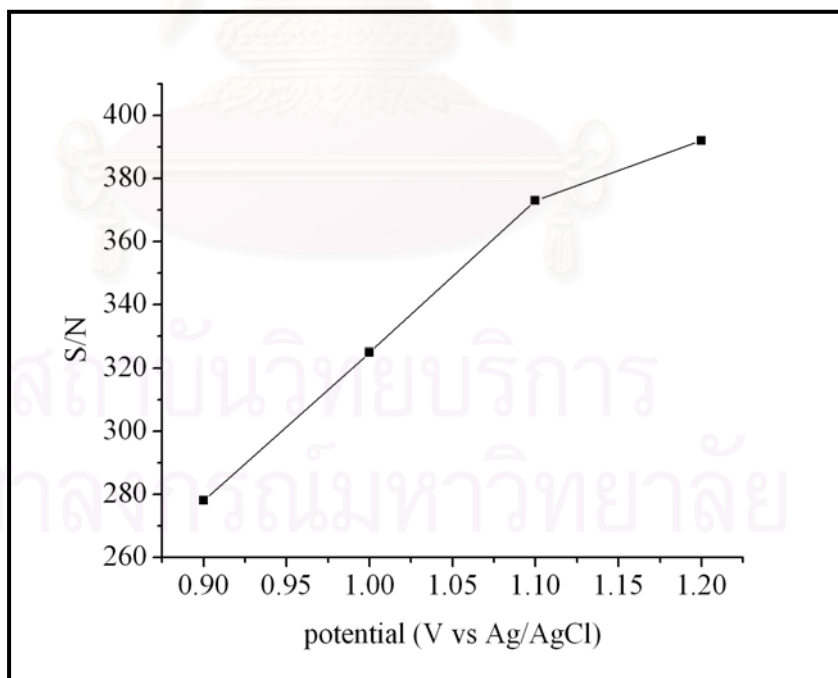


Figure 4-16 FI-PAD-BDD response as a function of E_{oxd} for 100 mg/L of iodide at the boron-doped diamond electrode.

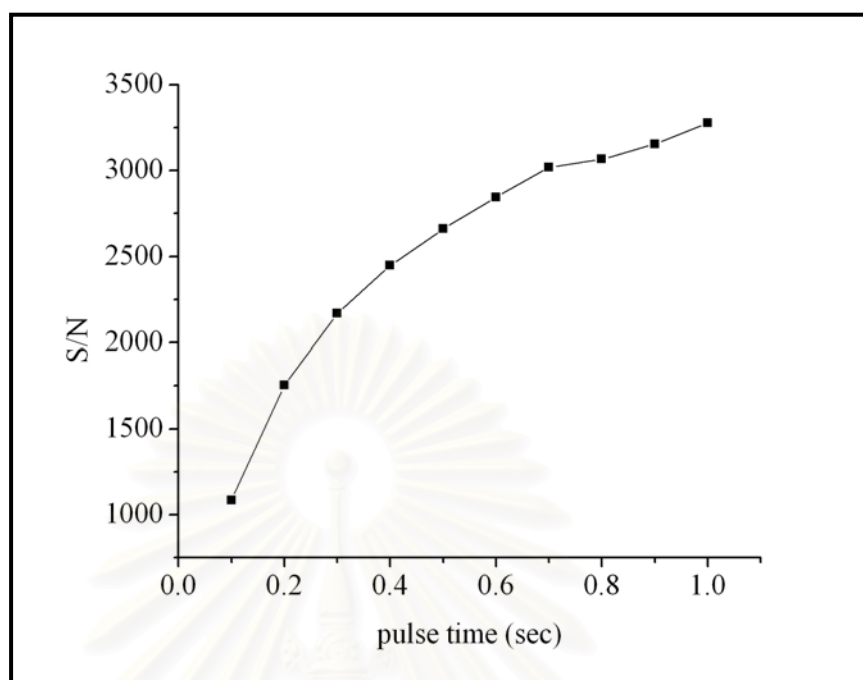


Figure 4-17 FI-PAD-BDD response as a function of t_{oxd} for 100 mg/L of iodide at the boron-doped diamond electrode.

Because of the formation of oxide on the electrode surface, it was essential that the E_{red} and t_{red} were optimized to achieve complete reductive dissolution of the surface oxide [25]. In the reactivation step, the reduction potential (E_{red}) was varied from +0.2 to +1.1 V versus Ag/AgCl. The detection potential (E_{det}), delay time (t_{del}), integration time (t_{int}), oxidation potential (E_{oxd}), oxidation time t_{oxd} and reduction time (t_{red}) were kept constant at 0.8 V, 30 msec, 30 msec, 1.2 V, 700 msec and 200 msec, respectively. The signal to noise ratio were obtained and the result was shown in Figure 4-18. The variation of reduction time (t_{red}) was optimized from 30 to 300 msec. The detection potential (E_{det}), delay time (t_{del}), integration time (t_{int}), oxidation potential (E_{oxd}), oxidation time t_{oxd} and reduction potential (E_{red}) were kept constant at 0.8 V, 30 msec, 30 msec, 1.2 V, 700 msec and 1.1 V, respectively. The signal to noise ratio were obtained and the result was shown in Figure 4-19.

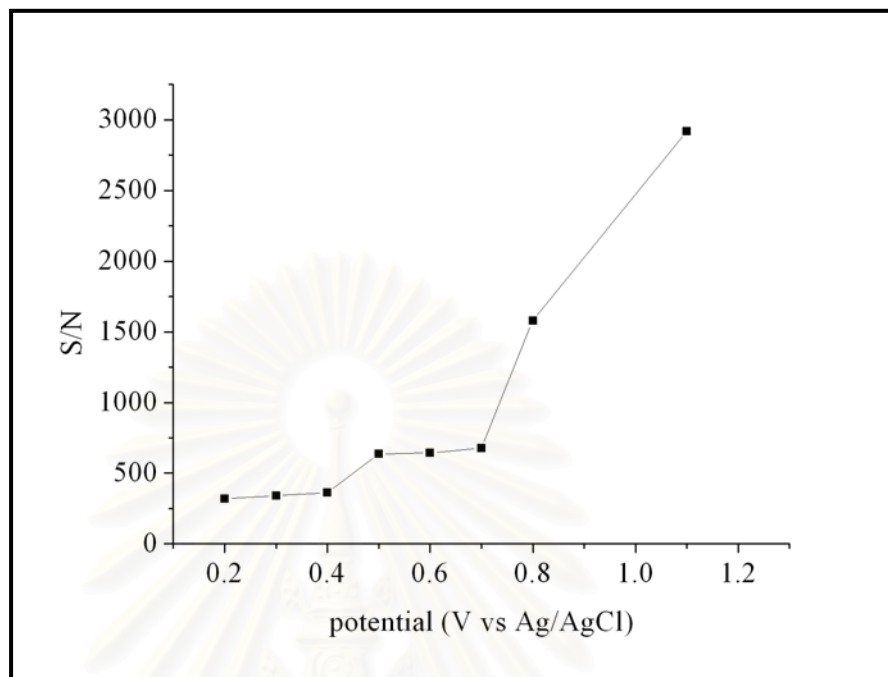


Figure 4-18 FI-PAD-BDD response as a function of E_{red} for 100 mg/L of iodide at the boron-doped diamond electrode.

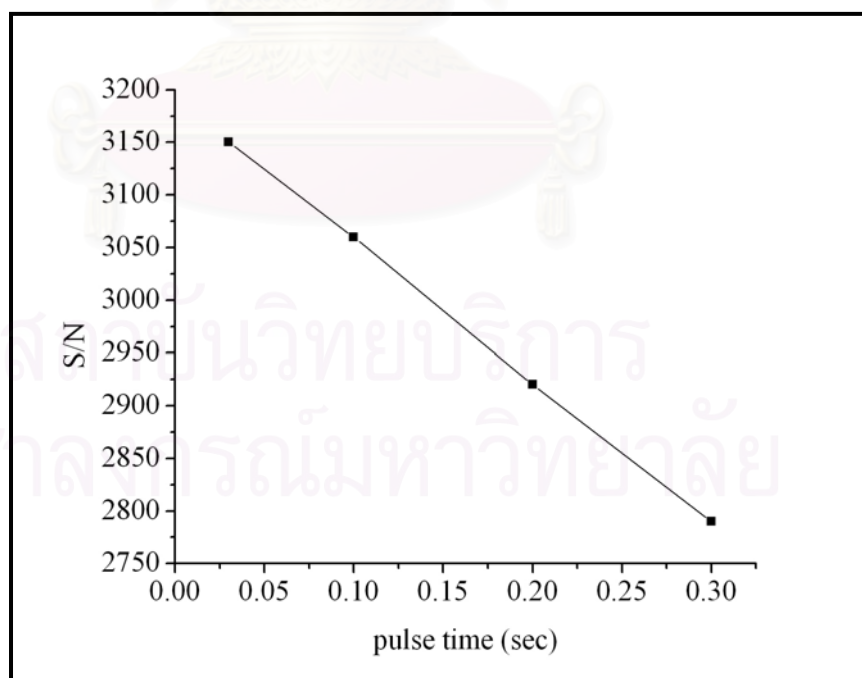


Figure 4-19 FI-PAD-BDD response as a function of t_{red} for 100 mg/L of iodide at the boron-doped diamond electrode.

The optimal PAD waveform parameters for iodide were summarized in Table 4-1 and were shown in Figure 4-20. The first step of cycle is the equilibration period, when the electrode is stabilized after the previous pulse [26]. The second step is the detecting step when the output from the detector is saved as data. The third step is the cleaning step when any compounds adhering to the electrode surface are oxidized at higher potential. The final step is the reduction step when the oxide is reduced. Then the next cycle begins.

Table 4-1 Optimal PAD waveform parameters for FI-PAD-BDD.

Parameter	Optimum
1. Detection step	
E_{det} (V vs. Ag/AgCl)	0.8
t_{del} (msec)	30
t_{int} (msec)	30
2. Oxidation step	
E_{oxd} (V vs. Ag/AgCl)	1.2
t_{oxd} (msec)	700
3. Reduction step	
E_{red} (V vs. Ag/AgCl)	1.1
t_{red} (msec)	30

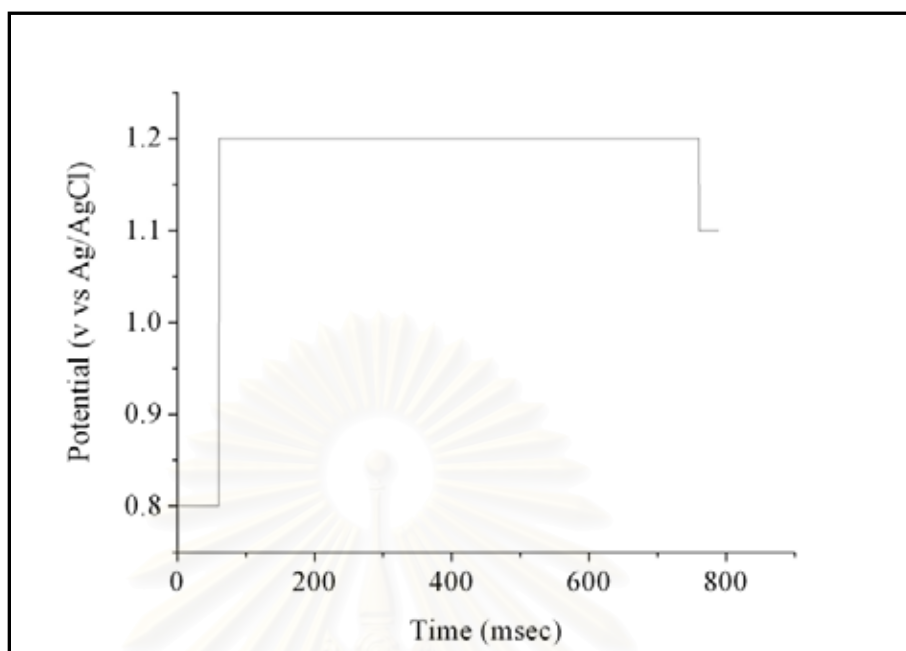


Figure 4-20 The three-step PAD waveform for the determination of iodide ion.

4.1.3.2 Method evaluation for flow injection analysis with pulsed amperometry using boron-doped diamond electrode (FI-PAD-BDD)

The method linearity between the current responses of iodide and iodide concentrations ranging from 50 to 2000 $\mu\text{g/L}$ was studied. Figure 4-21 showed the plot of the height of peak currents versus iodide concentrations. A linear dynamic range of 50 to 2000 $\mu\text{g/L}$ was observed correlation coefficient, $R^2 = 0.9942$. The limit of detection of 5.4 $\mu\text{g/L}$ and the limit of quantitation of 16.5 $\mu\text{g/L}$ were determined from 6 replicate injections of reagent blank. The recovery was 114% with 3% (N=3) using 500 $\mu\text{g/L}$ standard iodide solution.

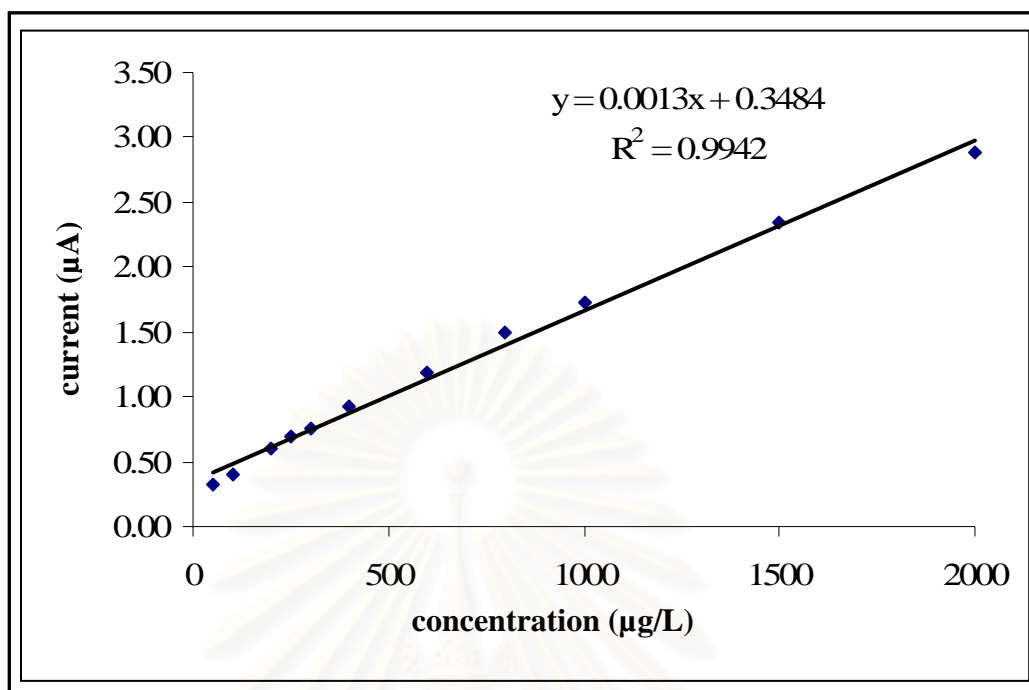


Figure 4-21 Linear dynamic range of iodide determined by FI-PAD-BDD.

4.2 Catalytic colorimetric method

4.2.1 Method evaluation for catalytic colorimetric method

The method linearity between the current responses of iodide and iodide concentrations ranging from 4 to 20 µg/L was studied. Figure 4-22 showed the plot of the height of peak currents versus iodide concentrations. A working range of 4 to 20 µg/L was observed and was represented by the linear regression equation: $y = -0.0285x + 0.7928$ with correlation coefficient, $R^2 = 0.9979$. The limit of detection of 0.7 µg/L and the limit of quantitation of 1.7 µg/L were determined from 6 replicate injections of reagent blank. The recovery was 117% with 1% (N=3) using 8 µg/L standard iodide solution.

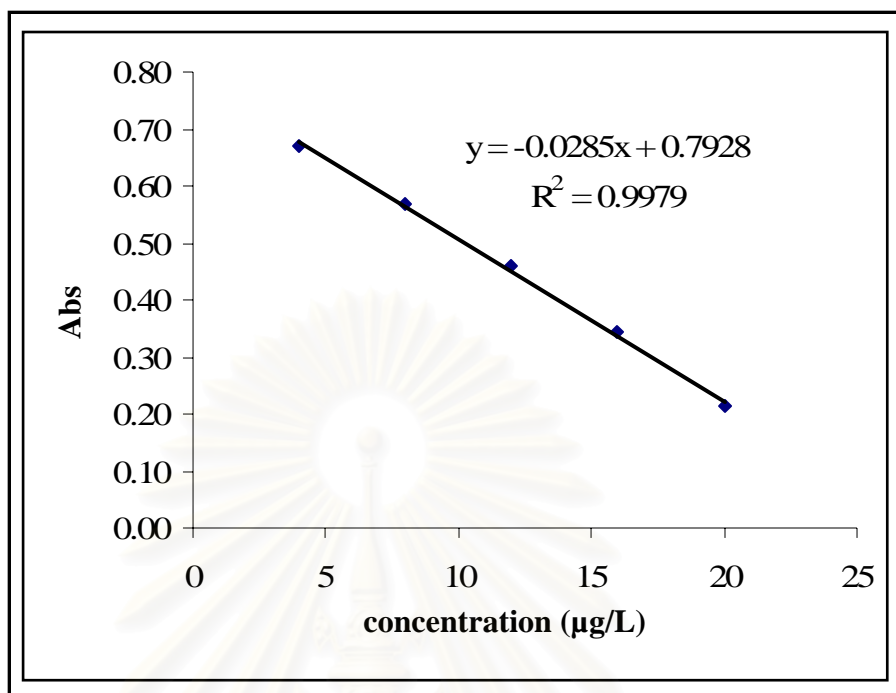


Figure 4-22 Working range of iodide determined by catalytic colorimetric method.

4.3 Application of electrochemical techniques for determination of iodide in egg sample

The electrochemical methods were attempted to apply for determination of iodide in egg samples. Unfortunately, the sample matrices after sample preparation step for which alkali dry ashing was used, were incompatible with the electrochemical techniques. The sample matrices were highly basic, which were inappropriate for electrochemical reaction of iodide. Moreover, the ashing residue might cause some clogging to the injection valve in the flow injection system. The samples need to be neutralized and filtered that might lead to losses and contamination. Alternatively, microdialysis sampling was employed for retrieving iodide ion from egg samples. Since the microdialysis sampling was introduced in this work and not in the main objective in the first place, the optimum conditions for the microdialysis sampling were not studied at this time. However, the comparative results of using microdialysis sampling with electrochemical methods were preliminarily investigated and summarized in Table 4-2.

4.3.1 Microdialysis sampling [29-31]

Since there was a technical problem with the application of electrochemical techniques to egg sample after alkali dry ashing due to that the matrix of the solution was incompatible to the electrochemical system, microdialysis sampling was used for sample preparation of iodide from egg sample. The technical set up of microdialysis system was illustrated in Figure 4-23. The microdialysis process was carried out via 10 cm polysulfone hollow fiber membrane inserting into approximately 50 g of homogenized egg sample in a HDPE bottle. The 50 mL of 60 mM phosphate buffer pH 5 was used as perfusate flowing and circulating inside the hollow fiber membrane at 1 mL/min for 1 hr.

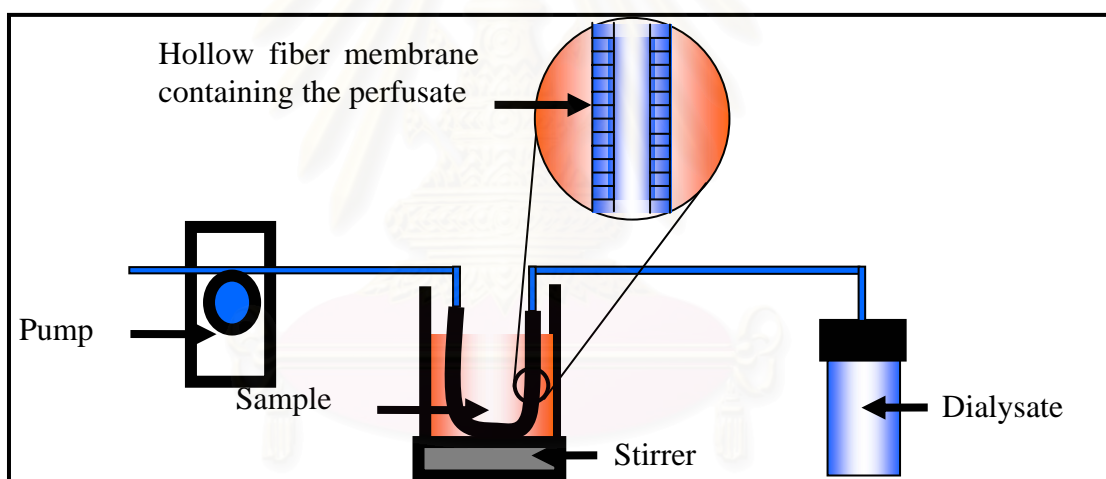


Figure 4-23 Technical setup of hollow fiber membrane microdialysis system.

Table 4-2 Comparative results of flow injection-electrochemical methods and catalytic colorimetric method for determination of iodide in egg samples.

Evaluation Method	FI- ampero-BDD	FI- PAD-BDD	Catalytic colorimetric method
Linear dynamic range	30-100 mg/L	50-2000 μ g/L	4-20 ^a μ g/L
R ²	0.9974	0.9942	0.9979
LOD	12.7 mg/L	5.36 μ g/L	0.68 μ g/L
LOQ	28.37 mg/L	16.54 μ g/L	1.74 μ g/L
%recovery (%RSD)*	91 (9)	114 (6)	117 (1)
Iodide in egg (%RSD)**	N/A	1.06 μ g/g (6)	1.11 μ g/g (0.1)

^a Working range

N/A – not available

* N=3

** N=4

From Table 4-2, the flow injection analysis with amperometric detection using boron-doped diamond was observed the linear range, LOD and LOQ in the higher concentration level. This method cannot be used in the lower concentration level. In addition, the repeatability of the method and life time of BDD electrode decreased it could be the adsorption of product or complex matrix occurs on the BDD electrode surface. Pulsed amperometric detection was widely used for cleaning and improving reproducible electrode activity [25-26]. The catalytic colorimetric method gave the better LOD and LOQ than the FI-PAD-BDD. However, the FI-PAD-BDD gave the wider linear dynamic range than other method it can be used in the lower level similarly to the catalytic colorimetric method. The FI-PAD-BDD gave the precision and accuracy similarly to the catalytic colorimetric method. It can be expected that the FI-PAD-BDD may be applied for the determination of iodide ion in egg samples.

The FI-PAD-BDD was applied for the determination of iodide in egg samples and result was compared with that obtained by catalytic colorimetric method. The sample solution was injected under the same condition as that of the standards solution. The iodide concentration was calculated from calibration equation and was 1.06 $\mu\text{g/g}$ of egg with 6%RSD (N=4). The catalytic colorimetric method was applied for the determination of iodide in egg sample. The iodide concentration was calculated from calibration equation and was 1.11 $\mu\text{g/g}$ of egg with 0.1% RSD (N=4). The FI-PAD-BDD was successfully applied for determination of iodide in egg samples, eliminated the adsorption on BDD electrode surface, increased life time of BDD electrode and decreased LOD and LOQ.

The systematic error was studied to confirm that it was real iodide signal. The experiment was performed by spiked 20 $\mu\text{g/g}$ standard iodide solution and 100 $\mu\text{g/g}$ standard iodide solutions into egg samples. The results were compared. The signal of spiked 20 $\mu\text{g/g}$ standard iodide solution was 3.00 $\mu\text{g/g}$ of egg with 9.70% recovery (6%RSD, n=4). The signal of spiked 100 $\mu\text{g/g}$ standard iodide solution was 11.54 $\mu\text{g/g}$ of egg with 8.54% recovery (2%RSD, n=4). From the results, it could confirm that the signal from FI-PAD-BDD was real iodide signal. The recovery was 8 to 10 %r, which could be the effect of microdialysis sampling. The optimum condition for the microdialysis sampling would be further studied.

CHAPTER V

CONCLUSION AND SUGGESTION OF FUTURE WORK

5.1 Conclusion

The electrochemical techniques were developed for determination of iodide ion in egg samples. The electrochemical reaction of iodide was investigated at BDD electrode and GC electrode by cyclic voltammetry. It was found that the iodide provided well-defined cyclic voltammograms at both electrodes. However, the background current of BDD electrode was much lower than the background current of GC electrode. Therefore, the BDD electrode was chosen for this work.

The optimal potential of flow injection analysis with amperometric detection was studied by hydrodynamic Voltammetry at BDD electrode by the flow injection analysis. The flow injection analysis condition was carried out using the mobile phase of phosphate buffer (60 mM, pH 5) at a flow rate of 1.0 mL/min at room temperature. The method evaluation of flow injection analysis with amperometric detection using boron-doped diamond were obtained the linear dynamic range, LOD and LOQ in the higher concentration level, hence flow injection analysis with amperometric detection using boron-doped diamond cannot be used in the lower concentration level. In addition, the repeatability of the method and life time of BDD electrode decreased when used this method for the determination of iodide ion in egg samples. It could be the adsorption of product or complex matrix occurs on the BDD electrode surface.

Pulsed amperometric detection was widely used for cleaning and improving reproducible electrode activity. The PAD waveform parameters including E_{del} , t_{del} , t_{int} , E_{oxd} , t_{oxd} , E_{red} and t_{red} were optimized at BDD electrode by flow injection analysis. The flow injection analysis condition was carried out using the mobile phase of phosphate buffer (60 mM, pH 5) at a flow rate of 1.0 mL/min at room temperature. The method evaluation of FI-PAD-BDD was obtained the concentration level of linear dynamic range, LOD and LOQ similarly to the catalytic colorimetric method and the wider linear dynamic range than the catalytic colorimetric method.

The electrochemical methods were attempted to apply for determination of iodide in egg samples. Unfortunately, the sample matrices after sample preparation step for which alkali dry ashing was used, were incompatible with the electrochemical techniques. The sample matrices were highly basic, which were inappropriate for electrochemical reaction of iodide. Moreover, the ashing residue might cause some clogging to the injection valve in the flow injection system. The samples need to be neutralized and filtered, which might lead to losses and contamination. Alternatively, microdialysis sampling was employed for retrieving iodide ion from egg samples. Since the microdialysis sampling was introduced in this work and not in the main objective in the first place, the optimum conditions for the microdialysis sampling do not studied at this time. However, the comparative results of using microdialysis sampling with electrochemical methods were preliminarily investigated.

The FI-PAD-BDD was applied to egg sample and the result was compared with the catalytic colorimetric method. The FI-PAD-BDD and catalytic colorimetric method were 1.06 $\mu\text{g/g}$ of egg with 6%RSD for 4 duplicate of sample solution and 1.11 $\mu\text{g/g}$ of egg with 0.1% RSD for 4 replicate of sample solution, respectively. From the results, the FI-PAD-BDD was similarly to the catalytic colorimetric method. The systematic error was studied to confirm that was real iodide signal. The advantage of FI-PAD-BDD over the catalytic colorimetric method was the wider linear dynamic range.

5.2 Suggestion of future work

Since, the FI-PAD-BDD has been applied with microdialysis sampling for determination of iodide in egg samples, the effect of microdialysis sampling conditions shall be studied, such as the extraction fraction (EF), permeability factors, temperatures stability, performances and characteristics of hollow fiber membrane. Furthermore, the microdialysis sampling can be developed for online system with FI-PAD-BDD and can be developed for automatic system with sequential injection analysis (SIA).

REFERENCES

- (1) Edmonds, J.S. and Morita, M. The determination of iodine species in environmental and biological samples (Technical Report). *International Union of Pure and Applied Chemistry*. 1998, 70(8): 1567-1584.
- (2) Bruggink, C.; Rossum, W.J.M.; Spijkerman, E. and Beelen, E.S.E. Iodide analysis by anion-exchange chromatography and pulsed amperometric detection in surface water and adsorbable organic iodide. *Journal of Chromatography A*. 2007, 1144(2): 170-174.
- (3) Choengchan, N.; Uraisin, K.; Choden, K.; Veerasai, W.; Grudpan, K. and Nacapricha, D. Simple flow injection system for colorimetric determination of iodate in iodized salt. *Talanta*. 2002, 58(6): 1195-1201.
- (4) Fecher, P.A.; Goldmann, I. and Nagengast, A. Determination of iodine in food samples by inductively coupled plasma mass spectrometry after alkaline extraction. *Journal of Analytical Atomic Spectrometry*. 1998, 13(9): 977-982.
- (5) Geddes, C.D. Optimal thin film polymeric sensors for the determination of aqueous chloride, bromide and iodide ions at high pH, based on the quenching of fluorescence of two acridinium dyes. *Dyes and Pigments*. 2000, 45(3): 243-251.
- (6) Jakmunee, J. and Grudpan, K. Flow injection amperometry for the determination of iodate in iodized tablet salt. *Analytica Chimica Acta*. 2001, 438(1-2): 299-304.
- (7) Larsen, E.H. and Ludwigsen, M.B. Determination of iodine in food-related certified reference materials using wet ashing and detection by inductively coupled plasma mass spectrometry. *Journal of Analytical Atomic Spectrometry*. 1997, 12(4): 435-439.
- (8) De Araujo Nogueira, A.R.; Mockiuti, F.; De Souza, G.B. and Primavesi, O. Flow injection spectrophotometric catalytic determination of iodine in milk. *Analytical Sciences*. 1998, 14(3): 559-564.
- (9) Yang, R.H. Development of an iodine sensor based on fluorescence energy transfer. *Analyst*. 2000, 125(8): 1441-1445.

- (10) Yang, S.; Fu, S. and Wang, M. Determination of trace iodine in food and biological samples by cathodic stripping voltammetry. *Analytical Chemistry*. 1991, 63(24): 2970-2973.
- (11) Das, P.; Gupta, M.; Jain, A. and Verma, K.K. Single drop microextraction or solid phase microextraction-gas chromatography-mass spectrometry for the determination of iodine in pharmaceuticals, iodized salt, milk powder and vegetables involving conversion into 4-iodo-N,N-dimethylaniline. *Journal of Chromatography A*. 2004, 1023(1): 33-39.
- (12) Schwehr, K.A. and Santschi, P.H. Sensitive determination of iodine species, including organo-iodine, for freshwater and seawater samples using high performance liquid chromatography and spectrophotometric detection. *Analytica Chimica Acta*. 2003, 482(1): 59-71.
- (13) Bermejo-Barrera, P.; Abola-Somoza, M. and Bermejo-Barrera, A. Atomic absorption spectrometry as an alternate technique for iodine determination (1968-1998). *Journal of Analytical Atomic Spectrometry*. 1999, 14(7): 1009-1018.
- (14) Ratanawimarnwong, N.; Amornthammarong, N.; Choengchan, N.; Chaisuwan, P.; Amatathongchai, M.; Wilairat, P.; McKelvie, I.D. and Nacapricha, D. Determination of iodide by detection of iodine using gas-diffusion flow injection and chemiluminescence. *Talanta*. 2005, 65(3): 756-761.
- (15) Choengchan, N.; Lukkanakul, K.; Ratanawimarnwong, N.; Waiyawat, W.; Wilairat, P. and Nacapricha, D. Use of pseudo-first order kinetics in flow injection for determination of trace inorganic iodine. *Analytica Chimica Acta*. 2003, 499(1-2): 115-122.
- (16) Moxon, R.E. and Dixon, E.J. Semi-automatic method for the determination of total iodine in food. *Analyst*. 1980, 105: 344-352
- (17) Moxon, R.E. Automatic methods for the determination of total inorganic iodine and free iodide in waters. *Analyst*. 1984, 109: 425-430.
- (18) Garwin, J.L.; Rosenholtz, N.S. and Abdollahi, A. Two colorimetric Assays for iodine in foods. *Journal of Food Science*. 1994, 59(5): 1135-1143.

- (19) Yao, S.; Chen, P. and Wei, W. A quartz crystal microbalance method for the determination of iodine in foodstuffs. *Food Chemistry*. 1999, 67(3): 311-316.
- (20) Pungor, E. The theory of ion-selective electrodes. *Analytical Sciences*. 1998, 14(2): 249-256.
- (21) Lefevre, G.; Bessiere, J. and Walcarius, A. Cuprite-modified electrode for the detection of iodide species. *Sensors and Actuators B*. 1999, 59: 113-117.
- (22) Chailapakul, O.; Amatathongchai, M.; Wilairat, P.; Grudpan, K. and Nacapricha, D. Flow-injection determination of iodide ion in nuclear emergency tablets, using boron-doped diamond thin film electrode. *Talanta*. 2004, 64(5): 1253-1258.
- (23) Monk, P.M.S. *Electroanalytical Chemistry*. 2001. New York: John Wiley and Sons.
- (24) Wang, J. *Analytical Electrochemistry*. 2nd ed. New York: John Wiley and Sons.
- (25) Johnson, D.C. and LaCourse, W.R. Liquid chromatography with pulsed electrochemical detection at gold and platinum electrodes. *Analytical Chemistry*. 1990, 62(10).
- (26) Long, C.; Yang, X.; Lee, B. and Ong, C. Optimizing the triple-potential waveform for the pulsed amperometric detection of streptomycin. *Analytical Letters*. 2005, 38: 1759-1767.
- (27) Wongkhan, K. "The kinetic study of iodide catalysed reaction between iron (III)-thiocyanate complex ion by nitrate and nitrite in sulfuric acid" (Master of science, Graduate School, Mahidol University, 2003).
- (28) Martin, H.B.A.; Landau, U.; Anderson, A.B. and Angus, J.C. Hydrogen and oxygen evolution on boron-doped diamond electrodes. *Journal of Electrochemical Society*. 1996, 143:133-136.
- (29) Lin, C.; Sheu, J.; Wu, H. and Huang, Y. Determination of hydroquinone in cosmetic emulsion using microdialysis sampling coupled with high performance liquid chromatography. *Journal of Pharmaceutical and Biomedical Analysis*. 2005, 38(3): 414-419.

- (30) Torto, N.; Bang, J.; Richardson, S.; Nilsson, G.S.; Gorton, L.; Laurell, T. and Marko-Varga, G. Optimal membrane choice for microdialysis sampling of oligosaccharides. *Journal of Chromatography A*. 1998, 806(2): 265-278.
- (31) Torto, N. and Laurell, T. Microdialysis sampling challenges and new frontiers. *LC-GC Europe*. 2001.
- (32) Ruzicka, J. and Hansen, E.H. *Flow injection analysis*. 2nd ed. New York: John Wiley and Sons.



สถาบันวิทยบริการ
จุฬาลงกรณ์มหาวิทยาลัย



สถาบันวิทยบริการ
จุฬาลงกรณ์มหาวิทยาลัย

Table A-1 The current responds of optimization pH by cyclic voltammetry using BDD electrode.

	Oxidation				Reduction			
	triiodide		iodine		triiodide		iodine	
	E/V	i/ μ A	E/V	i/ μ A	E/V	i/ μ A	E/V	i/ μ A
pH3	0.586	17.81	0.869	11.36	0.522	-20.48	0.801	-2.755
	0.591	17.14	0.869	12.08	0.522	-20.62	0.801	-3.548
	0.591	16.75	0.659	10.18	0.522	-13.47	0.583	-10.83
pH4	0.596	18.02	0.825	10.89	0.522	-19.68	0.742	-4.032
	0.593	17.66	0.825	11.23	0.522	-19.38	0.745	-4.127
	0.591	17.54	0.654	11.63	0.52	-14.02	0.571	-11.88
pH5	0.593	17.66	0.764	9.74	0.522	-16.66	0.676	-5.619
	0.588	17.07	0.764	8.85	0.522	-16.98	0.679	-5.761
	0.588	15.29	0.647	7.932	0.525	-11.53	0.564	-10.52
pH6	0.598	17.87	0.679	8.69	0.53	-15.33	0.605	-9.462
	0.598	17.93	0.684	10.14	0.527	-13.84	0.605	-9.499
	0.593	18.14	0.635	5.481	0.527	-7.504	N/A	N/A
pH7	0.591	13.69	0.620	5.55	0.53	-20.49	N/A	N/A
	0.596	14.75	0.613	6.02	0.535	-19.45	N/A	N/A
	0.591	16.84	0.627	6.64	0.527	-19.46	N/A	N/A
pH8	0.652	27.60	N/A	N/A	0.537	-22.55	N/A	N/A
	0.642	27.90	N/A	N/A	0.535	-23.35	N/A	N/A
	0.600	26.87	N/A	N/A	0.532	-20.64	N/A	N/A

N/A – not available due to I_3^- and I_2 were overlapped.

Table A-2 The current responds of optimization pH by cyclic voltammetry using GC electrode.

	Oxidation				Reduction			
	triiodide		iodine		triiodide		iodine	
	E/V	i/ μ A	E/V	i/ μ A	E/V	i/ μ A	E/V	i/ μ A
pH 3	0.491	16.42	0.686	13.51	0.420	-15.47	0.603	-10.93
	0.491	16.53	0.684	12.32	0.420	-14.49	0.598	-10.58
	0.491	16.75	0.659	10.18	0.422	-13.47	0.583	-10.83
pH4	0.491	16.66	0.657	10.26	0.422	-12.69	0.574	-9.71
	0.491	17.54	0.654	11.63	0.420	-14.02	0.571	-11.88
	0.491	17.85	0.654	11.57	0.422	-12.69	0.571	-12.46
pH5	0.491	15.68	0.649	8.59	0.425	-11.20	0.571	-11.00
	0.488	15.29	0.647	7.93	0.425	-11.53	0.564	-10.52
	0.488	15.53	0.647	8.26	0.422	-11.53	0.564	-9.975
pH6	0.491	16.36	0.637	7.46	0.425	-9.78	N/A	N/A
	0.488	15.90	0.635	9.75	0.422	-11.58	N/A	N/A
	0.491	16.84	0.627	6.64	0.427	-8.767	N/A	N/A
pH7	0.583	24.22	N/A	N/A	0.432	-20.64	N/A	N/A
	0.576	24.15	N/A	N/A	0.432	-19.70	N/A	N/A
	0.566	23.65	N/A	N/A	0.432	-19.64	N/A	N/A
pH8	0.493	25.67	N/A	N/A	N/A	N/A	N/A	N/A
	0.503	26.93	N/A	N/A	N/A	N/A	N/A	N/A
	0.500	26.87	N/A	N/A	N/A	N/A	N/A	N/A

N/A – not available due to I_3^- and I_2 were overlapped.

Table A-3 The current responds of varies scan rate at BDD electrode.

scan rate mV/s	sca rate ^{1/2} (mV/s) ^{1/2}	Oxidation			
		triiodide		iodine	
		E/V	i/A	E/V	i/A
10	3.162	0.537	3.04	0.789	0.50
		0.537	3.04	0.789	0.50
		0.537	2.98	0.767	0.40
25	5.000	0.544	3.59	0.750	0.45
		0.544	3.59	0.750	0.45
		0.547	3.46	0.776	0.60
50	7.071	0.562	4.88	0.798	1.04
		0.562	4.88	0.798	1.04
		0.562	4.86	0.798	1.01
75	8.660	0.569	5.88	0.803	1.20
		0.569	5.88	0.803	1.20
		0.571	5.95	0.818	1.59
100	10.000	0.579	6.75	0.820	1.55
		0.579	6.75	0.820	1.55
		0.579	6.72	0.813	1.33
200	14.142	0.601	9.43	0.854	2.62
		0.601	9.43	0.854	2.62
		0.601	9.40	0.840	2.01
300	17.321	0.615	11.40	0.862	2.75
		0.615	11.40	0.862	2.75
		0.615	11.38	0.864	2.84
400	20.000	0.627	12.97	0.886	3.68
		0.627	12.97	0.886	3.68
		0.630	12.87	0.894	3.99

		Oxidation			
scan rate	sca rate ^{1/2}	triiodide		iodine	
mV/s	(mV/s) ^{1/2}	E/V	i/A	E/V	i/A
		0.640	14.06	0.896	3.42
500	22.361	0.640	14.06	0.896	3.42
		0.637	14.19	0.901	3.86

Table A-4 The current responds of varies scan rate at GC electrode.

		Oxidation			
scan rate	scan rate ^{1/2}	triiodide		iodine	
mV/s	(mV/s) ^{1/2}	E/V	i/μA	E/V	i/μA
		0.498	8.07	0.654	7.41
10	3.162	0.498	8.10	0.654	6.83
		0.498	8.29	0.652	7.32
		0.496	12.96	0.649	7.86
25	5.000	0.493	12.66	0.649	8.25
		0.493	12.71	0.649	8.68
		0.488	17.25	0.649	11.42
50	7.071	0.491	17.47	0.649	10.80
		0.491	17.63	0.645	8.41
		0.491	21.72	0.649	11.31
75	8.660	0.488	21.23	0.654	12.33
		0.488	21.26	0.652	12.29
		0.491	25.22	0.659	13.59
100	10.000	0.491	24.74	0.654	13.12
		0.488	25.01	0.657	12.53
		0.491	35.67	0.671	17.27
200	14.142	0.491	35.09	0.669	14.54
		0.491	36.14	0.671	14.39

scan rate mV/s	scan rate ^{1/2} (mV/s) ^{1/2}	Oxidation			
		triiodide		iodine	
		E/V	i/μA	E/V	i/μA
300	17.321	0.491	43.46	0.684	18.96
		0.493	44.31	0.684	15.16
		0.496	44.28	0.686	16.06
400	20.000	0.498	51.27	0.698	20.4
		0.496	51.28	0.698	19.61
		0.496	50.13	0.701	21.32
500	22.361	0.500	57.32	0.710	19.90
		0.500	56.98	0.710	19.75
		0.498	57.39	0.710	21.42

Table A-5 The current responds of hydrodynamic voltammetry for FI-amperometry with BDD electrode of 100 mg/L iodide in 60 mM phosphate buffer (pH 5) at various potentials.

Potential (V vs Ag/AgCl)	Noise (N/μA)	Signal current (S/μA)	S/N (μA)
0.3	0.0017	0.0197	11.5439
	0.0017	0.0201	11.6628
	0.0016	0.0225	14.0813
	0.0016	0.0219	13.6750
0.4	0.0031	0.0442	14.3636
	0.0029	0.0343	11.9547
	0.0027	0.0354	13.2547
	0.0027	0.0496	18.5149
0.5	0.0039	0.0670	17.0969
	0.0038	0.0595	15.4870
	0.0036	0.0641	17.8496
	0.0036	0.0611	17.0111

Potential (V vs Ag/AgCl)	Noise (N/ μ A)	Signal current (S/ μ A)	S/N (μ A)
0.6	0.0058	0.1215	20.9483
	0.0053	0.1301	24.5472
	0.0051	0.1797	35.5842
	0.0050	0.1926	38.5200
0.7	0.0107	4.0170	375.4206
	0.0098	4.2470	433.3673
	0.0094	4.2730	454.5745
	0.0089	4.2690	479.6629
0.8	0.0184	9.5270	517.7717
	0.0171	9.5810	560.2924
	0.0164	9.6940	591.0976
	0.0161	9.6640	600.2484
0.9	0.0324	14.9700	462.0370
	0.0292	14.9000	510.2740
	0.0278	14.8700	534.8921
	0.0266	14.8500	558.2707
1	0.0590	20.0900	340.5085
	0.0510	20.0900	393.9216
	0.0510	19.9800	391.7647
	0.0510	20.1000	394.1176
1.1	0.0940	25.3000	269.1489
	0.0810	25.2400	311.6049
	0.0760	25.2600	332.3684
	0.0720	25.4200	353.0556
1.2	0.1550	29.9700	193.3548
	0.1400	30.0600	214.7143
	0.1330	29.9500	225.1880
	0.1220	30.1700	247.2951

Table A-6 FI-PAD-BDD response as a function of t_{del} for 100 mg/L of iodide at the boron-doped diamond electrode.

time (msec)	Noise (N/ μ A)	Signal current (S/ μ A)	S/N (μ A)
200	0.0032	5.3040	1662.6959
	0.0032	5.3150	1666.1442
	0.0032	5.2960	1660.1881
	0.0032	5.2130	1634.1693
	0.0032	5.2560	1647.6489
	0.0032	5.0820	1593.1034
100	0.0032	5.9010	1849.8433
	0.0032	6.1050	1913.7931
	0.0032	5.6740	1778.6834
	0.0032	5.9810	1874.9216
	0.0032	6.1740	1935.4232
	0.0032	5.4090	1695.6113
90	0.0032	7.3600	2307.2100
	0.0032	7.2900	2285.2665
	0.0032	6.8520	2147.9624
	0.0032	6.9530	2179.6238
	0.0032	7.5470	2365.8307
	0.0032	7.5330	2361.4420
80	0.0032	7.9490	2491.8495
	0.0032	7.9220	2483.3856
	0.0032	7.8480	2460.1881
	0.0032	8.0570	2525.7053
	0.0032	7.5430	2364.5768
	0.0032	7.9640	2496.5517

time (msec)	Noise (N/ μ A)	Signal current (S/ μ A)	S/N (μ A)
70	0.0032	8.0430	2521.3166
	0.0032	8.4060	2635.1097
	0.0032	8.4170	2638.5580
	0.0032	7.7910	2442.3197
	0.0032	7.8390	2457.3668
	0.0032	8.3630	2621.6301
60	0.0032	8.5030	2665.5172
	0.0032	8.3170	2607.2100
	0.0032	8.3060	2603.7618
	0.0032	8.1060	2541.0658
	0.0032	8.6460	2710.3448
	0.0032	8.1640	2559.2476
50	0.0032	9.0630	2841.0658
	0.0032	8.9720	2812.5392
	0.0032	8.9490	2805.3292
	0.0032	9.0910	2849.8433
	0.0032	9.1070	2854.8589
	0.0032	8.9470	2804.7022
40	0.0032	9.5330	2988.4013
	0.0032	9.1420	2865.8307
	0.0032	9.1210	2859.2476
	0.0032	8.9140	2794.3574
	0.0032	9.6090	3012.2257
	0.0032	9.6130	3013.4796
30	0.0032	9.8410	3084.9530
	0.0032	10.1900	3194.3574
	0.0032	10.1600	3184.9530
	0.0032	10.2900	3225.7053
	0.0032	10.0600	3153.6050
	0.0032	10.3100	3231.9749

Table A-7 FI-PAD-BDD response as a function of t_{int} for 100 mg/L of iodide at the boron-doped diamond electrode.

time/msec	Noise (N/ μ A)	Signal current (S/ μ A)	S/N (μ A)
700	0.0032	1.8890	592.1630
	0.0032	2.1970	688.7147
	0.0032	2.1700	680.2508
	0.0032	2.0320	636.9906
	0.0032	1.9500	611.2853
	0.0032	1.8920	593.1034
500	0.0032	2.5160	788.7147
	0.0032	2.6840	841.3793
	0.0032	2.6220	821.9436
	0.0032	2.7460	860.8150
	0.0032	2.7270	854.8589
	0.0032	2.7000	846.3950
300	0.0032	3.9970	1252.9781
	0.0032	3.7790	1184.6395
	0.0032	3.9670	1243.5737
	0.0032	3.9610	1241.6928
	0.0032	3.8140	1195.6113
	0.0032	3.9160	1227.5862
100	0.0032	6.6380	2080.8777
	0.0032	6.7930	2129.4671
	0.0032	6.6780	2093.4169
	0.0032	6.8230	2138.8715
	0.0032	6.8260	2139.8119
	0.0032	6.7540	2117.2414

time (msec)	Noise (N/ μ A)	Signal current (S/ μ A)	S/N (μ A)
70	0.0032	7.6030	2383.3856
	0.0032	7.4300	2329.1536
	0.0032	7.6930	2411.5987
	0.0032	7.5080	2353.6050
	0.0032	7.5900	2379.3103
	0.0032	7.8250	2452.9781
30	0.0032	8.8440	2772.4138
	0.0032	8.7550	2744.5141
	0.0032	8.9930	2819.1223
	0.0032	8.8780	2783.0721
	0.0032	8.9570	2807.8370
	0.0032	9.0150	2826.0188

Table A-8 FI-PAD-BDD response as a function of E_{oxd} for 100 mg/L of iodide at the boron-doped diamond electrode.

Potential (V vs Ag/AgCl)	Noise (N/ μ A)	Signal current (S/ μ A)	S/N (μ A)
1.2	0.00319	1.151	360.815
	0.00319	1.186	371.7868
	0.00319	1.229	385.2665
	0.00319	1.188	372.4138
	0.00319	1.229	385.2665
	0.00319	1.187	372.1003
1.1	0.00319	1.129	353.9185
	0.00319	1.14	357.3668
	0.00319	1.147	359.5611
	0.00319	1.129	353.9185
	0.00319	1.12	351.0972
	0.00319	1.161	363.9498

Potential (V vs Ag/AgCl)	Noise (N/ μ A)	Signal current (S/ μ A)	S/N (μ A)
1	0.00319	1.03	322.884
	0.00319	0.9516	298.3072
	0.00319	0.9788	306.8339
	0.00319	0.9748	305.5799
	0.00319	0.9971	312.5705
	0.00319	1.025	321.3166
0.9	0.00319	0.8149	255.4545
	0.00319	0.8628	270.4702
	0.00319	0.8555	268.1818
	0.00319	0.8603	269.6865
	0.00319	0.8299	260.1567
	0.00319	0.8698	272.6646

Table A-9 FI-PAD-BDD response as a function of t_{oxd} for 100 mg/L of iodide at the boron-doped diamond electrode.

time/msec	Noise (N/ μ A)	Signal current (S/ μ A)	S/N (μ A)
1000	0.0032	2.1080	660.8150
	0.0032	2.2520	705.9561
	0.0032	2.2510	705.6426
	0.0032	2.1750	681.8182
	0.0032	2.1780	682.7586
	0.0032	2.1640	678.3699
900	0.0032	1.8090	567.0846
	0.0032	1.7870	560.1881
	0.0032	1.7600	551.7241
	0.0032	1.6780	526.0188
	0.0032	1.8520	580.5643
	0.0032	1.8110	567.7116

time/msec	Noise (N/ μ A)	Signal current (S/ μ A)	S/N (μ A)
800	0.0032	1.9200	601.8809
	0.0032	1.9100	598.7461
	0.0032	1.7460	547.3354
	0.0032	1.7750	556.4263
	0.0032	1.7120	536.6771
	0.0032	1.7980	563.6364
700	0.0032	1.8190	570.2194
	0.0032	1.8980	594.9843
	0.0032	1.8800	589.3417
	0.0032	1.8310	573.9812
	0.0032	1.8460	578.6834
	0.0032	1.8920	593.1034
600	0.0032	1.7840	559.2476
	0.0032	1.7850	559.5611
	0.0032	1.8180	569.9060
	0.0032	1.7870	560.1881
	0.0032	1.8250	572.1003
	0.0032	1.7370	544.5141
500	0.0032	1.7570	550.7837
	0.0032	1.6870	528.8401
	0.0032	1.7190	538.8715
	0.0032	1.5930	499.3730
	0.0032	1.6700	523.5110
	0.0032	1.6240	509.0909
400	0.0032	1.6410	514.4201
	0.0032	1.5870	497.4922
	0.0032	1.7180	538.5580
	0.0032	1.5910	498.7461
	0.0032	1.6950	531.3480
	0.0032	1.6920	530.4075

time/msec	Noise (N/ μ A)	Signal current (S/ μ A)	S/N (μ A)
300	0.0032	1.5110	473.6677
	0.0032	1.6270	510.0313
	0.0032	1.6170	506.8966
	0.0032	1.6200	507.8370
	0.0032	1.6080	504.0752
	0.0032	1.5380	482.1317
200	0.0032	1.4310	448.5893
	0.0032	1.3930	436.6771
	0.0032	1.4620	458.3072
	0.0032	1.4170	444.2006
	0.0032	1.4190	444.8276
	0.0032	1.4300	448.2759
100	0.0032	0.9188	288.0251
	0.0032	0.9125	286.0502
	0.0032	0.9615	301.4107
	0.0032	0.9918	310.9091
	0.0032	0.9310	291.8495
	0.0032	0.9430	295.6113

Table A-10 FI-PAD-BDD response as a function of E_{red} for 100 mg/L of iodide at the boron-doped diamond electrode.

Potential (V vs Ag/AgCl)	Noise (N/ μ A)	Signal current (S/ μ A)	S/N (μ A)
1.1	0.0032	8.8440	2772.4138
	0.0032	8.7550	2744.5141
	0.0032	8.9930	2819.1223
	0.0032	8.8780	2783.0721
	0.0032	8.9570	2807.8370
	0.0032	9.0150	2826.0188

Potential (V vs Ag/AgCl)	Noise (N/ μ A)	Signal current (S/ μ A)	S/N (μ A)
0.8	0.0032	4.8320	1514.7335
	0.0032	4.9040	1537.3041
	0.0032	4.9470	1550.7837
	0.0032	4.7540	1490.2821
	0.0032	4.8010	1505.0157
	0.0032	4.6120	1445.7680
0.7	0.0032	2.0360	638.2445
	0.0032	2.0660	647.6489
	0.0032	2.0990	657.9937
	0.0032	2.0900	655.1724
	0.0032	2.0970	657.3668
	0.0032	2.0230	634.1693
0.6	0.0032	1.8150	568.9655
	0.0032	1.9860	622.5705
	0.0032	1.9290	604.7022
	0.0032	1.9900	623.8245
	0.0032	2.0510	642.9467
	0.0032	2.0050	628.5266
0.5	0.0032	1.9520	611.9122
	0.0032	1.9110	599.0596
	0.0032	1.8920	593.1034
	0.0032	2.1810	683.6991
	0.0032	1.8070	566.4577
	0.0032	1.8870	591.5361
0.4	0.0032	1.1110	348.2759
	0.0032	1.1230	352.0376
	0.0032	1.1040	346.0815
	0.0032	1.1420	357.9937
	0.0032	1.0880	341.0658
	0.0032	1.0540	330.4075

Potential (V vs Ag/AgCl)	Noise (N/ μ A)	Signal current (S/ μ A)	S/N (μ A)
0.3	0.0032	1.0580	331.6614
	0.0032	1.0460	327.8997
	0.0032	1.0130	317.5549
	0.0032	1.0610	332.6019
	0.0032	1.0530	330.0940
	0.0032	1.0160	318.4953
0.2	0.0032	0.9040	283.3856
	0.0032	0.8902	279.0596
	0.0032	1.0740	336.6771
	0.0032	1.0110	316.9279
	0.0032	0.9583	300.4075
	0.0032	1.0310	323.1975

Table A-11 FI-PAD-BDD response as a function of t_{red} for 100 mg/L of iodide at the boron-doped diamond electrode.

time/msec	Noise (N/ μ A)	Signal current (S/ μ A)	S/N (μ A)
300	0.0032	8.2130	2574.6082
	0.0032	8.5780	2689.0282
	0.0032	8.6250	2703.7618
	0.0032	8.5490	2679.9373
	0.0032	8.6630	2715.6740
	0.0032	8.5520	2680.8777
200	0.0032	8.8440	2772.4138
	0.0032	8.7550	2744.5141
	0.0032	8.9930	2819.1223
	0.0032	8.8780	2783.0721
	0.0032	8.9570	2807.8370
	0.0032	9.0150	2826.0188

time/msec	Background current(B/ μ A)	Signal current(i/ μ A)	S/B (μ A)
100	0.0032	9.2610	2903.1348
	0.0032	9.2770	2908.1505
	0.0032	9.3270	2923.8245
	0.0032	9.3660	2936.0502
	0.0032	9.3950	2945.1411
	0.0032	9.3650	2935.7367
30	0.0032	9.6430	3022.8840
	0.0032	9.6090	3012.2257
	0.0032	9.6420	3022.5705
	0.0032	9.6680	3030.7210
	0.0032	9.4920	2975.5486
	0.0032	9.5860	3005.0157

สถาบันวิทยบริการ
จุฬาลงกรณ์มหาวิทยาลัย

VITA

Miss Piyada Suwandittakul was born on March 7, 1979 in Ratchaburi, Thailand. She received her Bachelor, degree of Education in Chemistry from Burapha University in 2001. After that she has been a graduated student at the Department of Chemistry Chulalongkorn University and become a member of Environmental Analysis Research Unit. She finished her Master's degree of Science in 2007.



สถาบันวิทยบริการ
จุฬาลงกรณ์มหาวิทยาลัย